# Referee1

Many thanks to the reviewer for the comments, and they have helped to improve the clarity of the manuscript. In the following, we address all the points raised in the review (denoted by italic letters). Text changes in the manuscript are highlighted in red or blue.

## 1. General comments

***The paper is an interesting and important contribution for assessment of the monsoon influence on the global stratosphere and should be published in ACP. New against earlier studies (e.g. Ploeger et al., 2017) is the analysis of NASM effects. However, the paper would gain a lot if simulations on the sensitivity of results on the positions of the boundaries of the monsoon boxes are included, especially the southern edge of ASM, which appears to be rather close to the equator, and the eastern edge of NASM (too far east). The position of the southern edge of ASM (e.g. 20N instead of 15N) might be critical for transport to the tropical pipe and to the southern hemisphere as indicated in Yu et al. (2017). This should be included in Figures 8 and 9. Also some sentences should address the differences to the method where the monsoon air masses are separated using PV instead of a rectangular box and if results are different to Garny and Randel (2016).***

A. Thanks for this important remark. We now added a sensitivity simulation with the ASM source region defined as [20° N, 45° N, 30° E, 120° E] and the NASM source region defined as [15° N, 40° N, 120° W, 60° W]. Figure RL 1 shows the average air mass fraction from ASM and NASM regions initialized in the 350−360 K and 370−380 K layers in July and August of 2010−2013 in the CLaMS-EI simulations during the following April−June. We can see a lot of similarities between Figure RL 1 and Fig.3 in the manuscript. In particular the transport patterns are not depending on the exact boundary of the source region. Here, more monsoon tracer is transported into the stratosphere from the 350−360 K layer than from the 370−380 K layer for both the ASM and NASM regions. The abundance of monsoon air initialized at 350−360 K is higher in the SH stratosphere than in the NH, while monsoon air initialized at 370−380 K is more likely to remain in the NH. The monsoon air mass in the stratosphere is lower than it from Fig.3 in the manuscript mainly because of the smaller domain used here.

To quantify the transport from source regions with different domain to the destination regions, we do the same as Fig.8 in the manuscript. Figure RL 2 shows CLaMS-EI time series of ASM and NASM tracer in the three destination regions (TrP, LS-NH and LS-SH). The abundances of ASM air in the three destination regions are slightly lower than those from Fig.8 in the manuscript as we expect because of the smaller domain. While the contributions from NASM to the LS-NH are much smaller compared to the results from Fig.8 in the manuscript because the domain used in the manuscript is almost twice larger than the domain here, we can see better comparison results from the transport efficiency (TE) below. However, the transport patterns are quite similar including the daily structures. Hence, the conclusions of our study are qualitatively robust to reasonable definition of the monsoon boundary.

Figure RL 3 compares the TE from the ASM and NASM source regions each divided into two layers (350−360 K and 370−380 K) to the three destination regions. Comparing the TE here and the TE from Fig.9 in the manuscript, we can see that the TEs from ASM/NASM to the three destination regions are

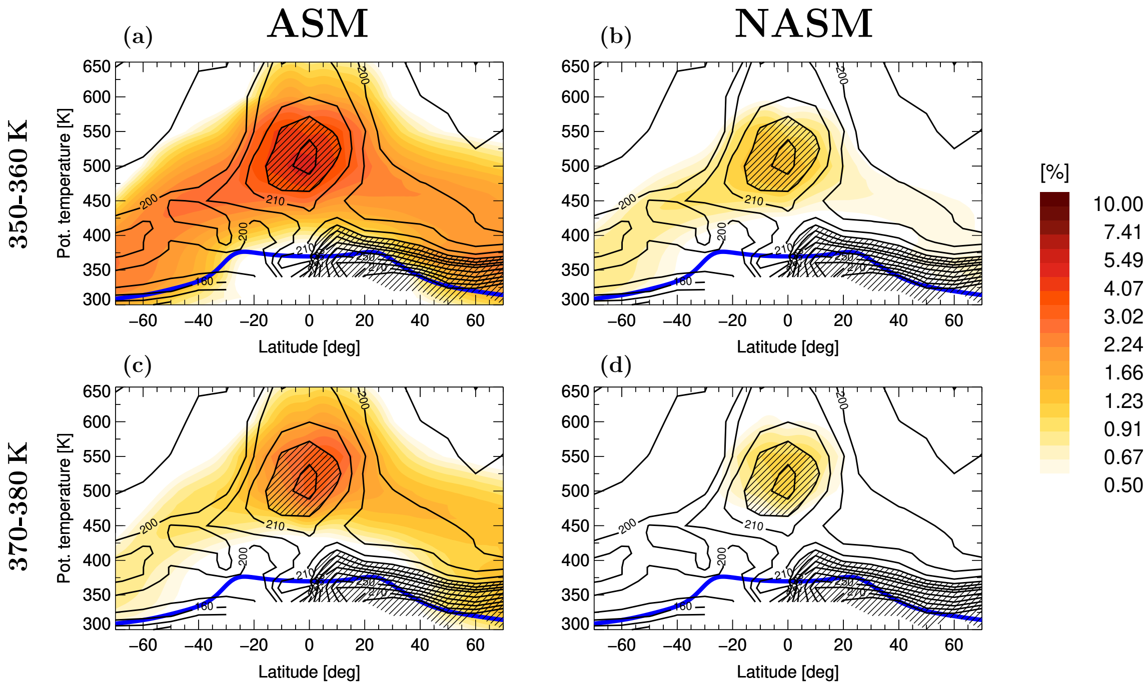


Figure RL 1: Climatological (2010−2013) zonal mean air mass fraction from the ASM (a and c) and the NASM (b and d) initialized at 350−360 K (upper) and 370−380 K (lower) in CLaMS-EI (color shading) during the following April−June. HCN from ACE-FTS observations (black contours) is also shown for context. Regions with HCN volume mixing ratios greater than 215 pptv are hatched. Blue lines mark the lapse rate tropopause. (Note the logarithmic color scale.)

slightly larger than those from Fig.9, especially for the NASM source region. The differences are small, we included a remark of this result in the discussion section (P22) of the manuscript instead of changing the figures.

Regarding the last point, the comparison results between our study and the results from Ploeger et al.(2017) and Garny and Randel (2016) are included in the revised version of the manuscript. There is good agreement with the work from Ploeger et al.(2017), we also include the difference in the manuscript. We can not compare the contributions of transport to different destinations from our study with the results from Garny and Randel (2016) because we use different method, and the meaning of the numbers in their work are also different from ours. The main comparison is related to the transport pathways to different destination regions from 360 K and 380 K. The insensitivity of the results to the source domain boundary in our study is in agreement with the findings shown by Garny and Randel (2016), where they found that the differences are small regarding a change in the source region definition from PV-contour to box.

## 2. Specific comments

(1) ***In Figure 1 it would be more useful to show CO for 350 or 360K. At 340K the reader is distracted by the large effects of biomass burning in the tropics.***

A. The CO at 350 K is shown in Fig.1, the text is changed correspondingly.

(2) ***Line 110: For clarity say 'tracer is reset to zero every...'. This should also go into the caption of Fig. 5.***

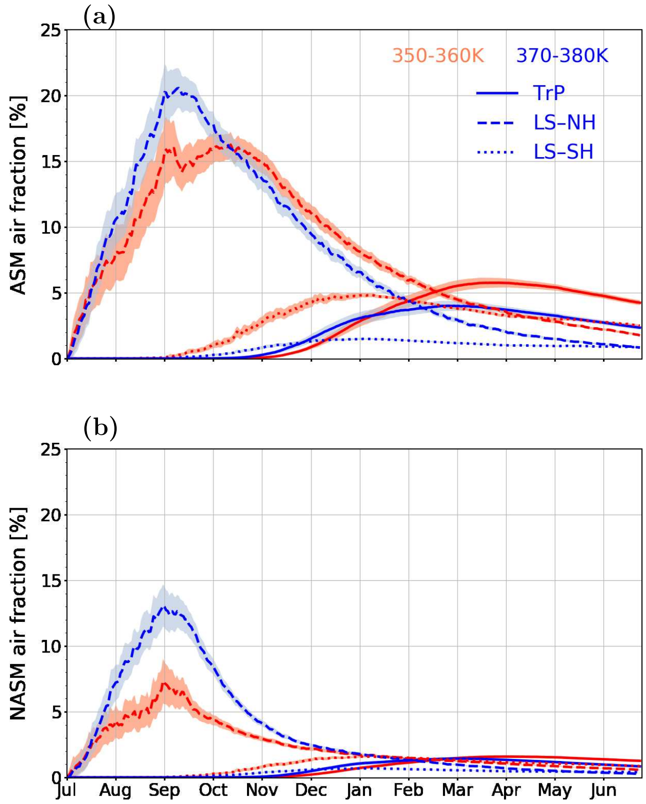


Figure RL 2: Climatological time series based on the CLaMS-EI simulations of source regions: (a) ASM and (b) NASM air mass fractions (in %) and diagnosed in three destination regions (see Fig.2 in the manuscript): tropical pipe (TrP, solid line), extratropical lower stratosphere in the NH (LS-NH, dashed line) and in the SH (LS-SH, dotted line). Shading shows the mean standard deviation in the zonal average (multiplied by 0.2 for better visibility). Red and blue lines respectively represent the tracers released in the 350−360 K and 370−380 K layer.

A. This is included in the caption of Fig.5 and Fig.6.

(3) ***Line 129ff: Please define more clearly on what the percentage mass fraction is based. Are the masses in the monsoon boxes during July and August 100%?***

A. The percentage mass fraction is based on the source air mass concentration (mixing ratio) in the stratosphere. Yes, the air masses in the monsoon boxes during July and August are 100%. The text is changed as well.

(4) ***Line 199: What is annual mean here? Is there each year different or is the mean of the 4-year time series meant? It might be sufficient just to show the MLS-data.***

A. The annual mean used here is different from each year. Figure RL 4 and Figure RL 5 respectively show the vertical and horizontal distribution of monsoon tracers together with the original MLS water vapor. We can see that the connection between monsoon tracers and MLS water vapor looks clear if we removed the annual mean.

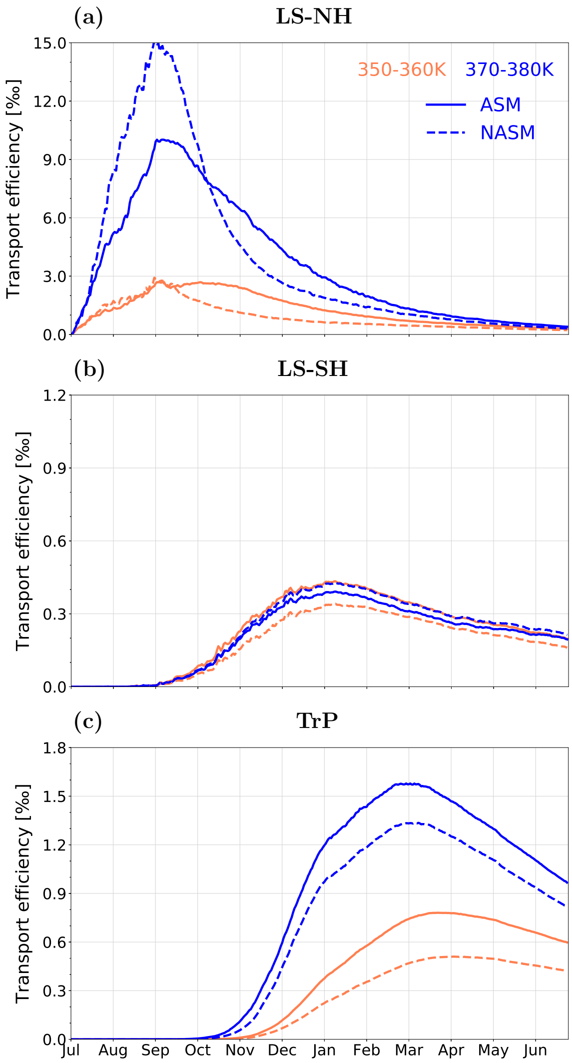


Figure RL 3: Climatological time series of transport efficiency (TE) as derived from the CLaMS-EI simulations and calculated for transport from the ASM (solid line)and NASM (dashed line) source regions to the (a) LS-NH , (b) LS-SH and (c) TrP destination regions. TE is defined by normalizing the average monsoon or tropical air mass over the destination region by the mass of the source region. Different colors of the lines represent tracers released at different levels.

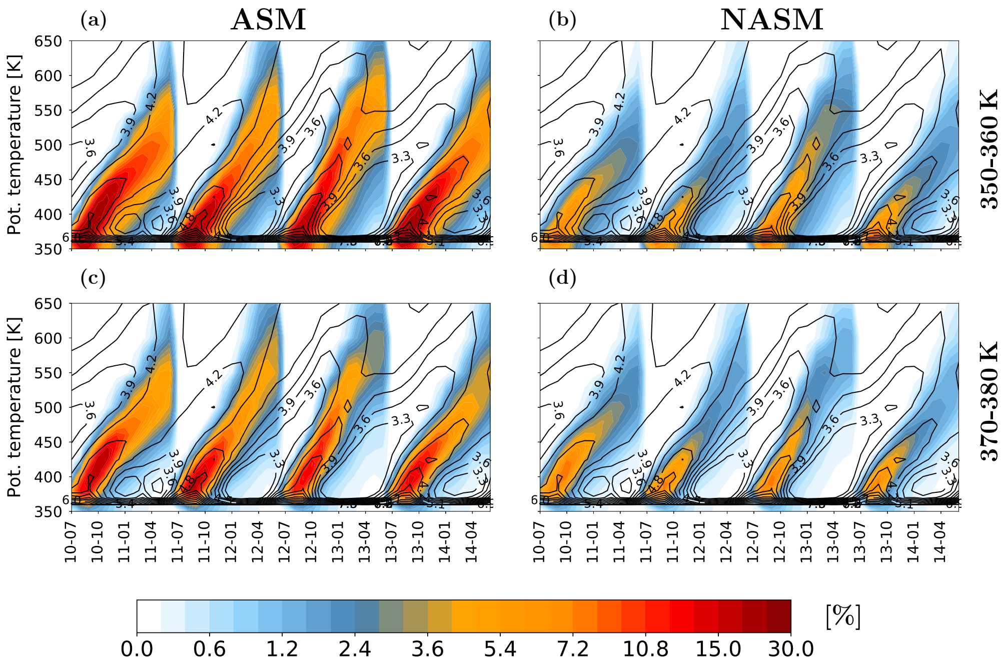


Figure RL 4: Potential temperature−time sections of mean monsoon air fraction (color shading) between 15° S and 15° N released in the 350−360 K (upper; a and b) and 370−380 K (lower; c and d) layers within the ASM (left; a and c) and NASM (right; b and d) based on CLaMS-EI simulations. Tape-recorder signals calculated from Aura MLS water vapor (in ppmv) are shown as black contours for context. Note that the tracer is set to zero everywhere on 1 July of each year.

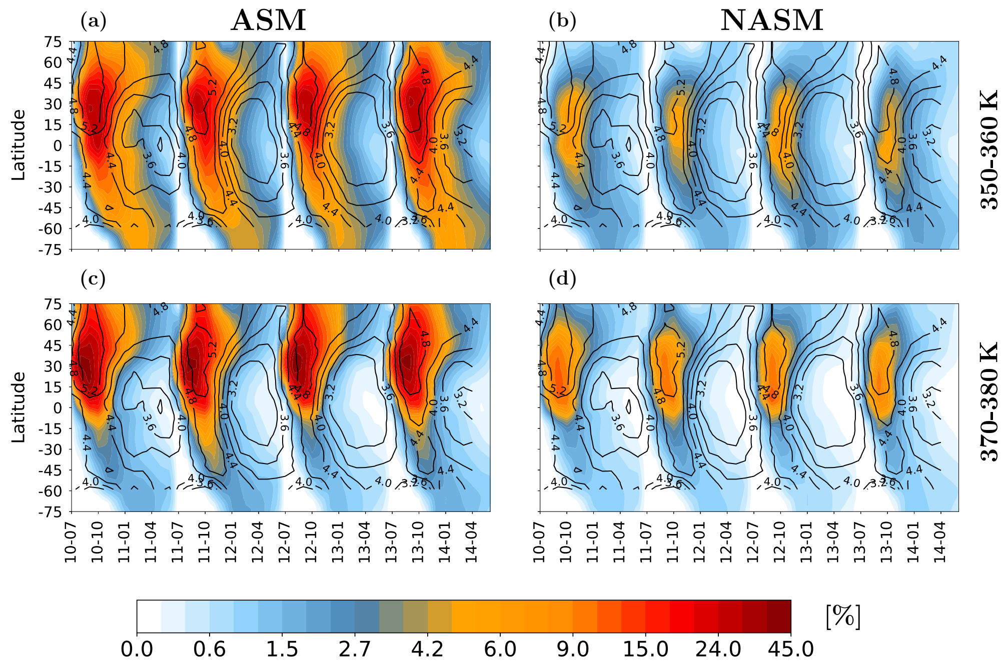


Figure RL 5: Zonal-mean tracer concentrations (color shading) for the ASM (left; a and c) and NASM (right; b and d) tracers initialized at 350−360 K (upper; a and b) and 370−380 K (lower; c and d) as functions of time and latitude on the 400 K isentropic surface based on CLaMS-EI. MLS water vapor retrievals (in ppmv) are shown as black contours for context. Note that the tracer is set to zero everywhere on 1 July of each year.

# 3. Technical corrections

(1) ***Line 17: Remove 'in contrast'.***

A. It is removed in the manuscript.

(2) ***Figure 1a: The rather arbitrary spacing of contours and colors should be more systematic (e.g. linear or a function mentioned in the caption) and fit to each other. Here also less colors are more.***

A. The colorbar and contour space are changed in Fig.1.

(3) ***Figure 3 and 4: Enhance sizes for legends and labels.***

A. The size of the legends and labels are enhanced in Fig.3 and Fig.4.

(4) ***Figure 5 and 6: Avoid smoothing artefact when tracer is reset, include 'zonal' in caption.***

A. The data is not smoothed. 'zonal' is included in the caption of Fig.5 and Fig.6.

(5) ***Check 'Competing interests'.***

A. 'Competing interests' is included in the manuscript.

(6) ***References: Correct Latex errors and remove second link for several entries.***

A. The errors about the references are corrected, and the second link of each citation is removed.

# Referee2

Many thanks to the reviewer for the comments, and they have helped to improve the clarity of the manuscript. In the following, we address all the points raised in the review (denoted by italic letters). Text changes in the manuscript are highlighted in red or blue.

## 1. General comments

(1) ***Somewhere in this manuscript (probably in multiple places, including the introduction, main discussion of results, and conclusions), the authors need to relate their findings to those of Vogel et al. [2019], who also used CLaMS artificial tracers to study transport of pollutants and the pathways by which air masses enter the tropical pipe via the ASM circulation. While that paper is cited as part of a list of references in the first paragraph of the Introduction, it is never mentioned again. Although the details of the two analysis approaches differ, I feel that some discussion of how the results from the current manuscript fit in with the concept of the "upward spiraling range" introduced by Vogel et al. [2019], as well as comparisons with the transit times and fraction of ASM air masses in the TrP that they calculated, is warranted here.***

A. Thanks for making us aware of this missing discussion. A more detailed comparison to the results of Vogel et al. [2019] is now included in the discussion section. The changes include comparable abundance of ASM air in the LS-NH from Vogel et al. [2019] (18% and 16% from 360 K and 380 K) and from our work (22% and 18%). The ASM air in the tropical pipe from Vogel et al. [2019] is 6%, which is also similar to our results (4%-6%). The transit time from ASM to the tropical pipe is about 8-9 months, which is consistent with the result from Vogel et al. [2019] with the transit time within ~1 year. The monsoon pathway from ASM at 350-360 K to the tropical pipe is inside the "upward spiraling range" introduced by Vogel et al. [2019], the tracers may transport upward in spiral rising way. However, the tracer setting between the work from Vogel et al. [2019] and our study is different, e.g. source regions, vertical range (boundary layer versus upper troposphere), and initialization periods (May-Oct versus Jul-Aug). Therefore the differences of the exact numbers are expected.

(2) ***The authors tend to cite one or two papers for well-established points, without adding "e.g." at the front of their short list. Obviously not all relevant papers can or even should be cited, but I feel that overlooking the literature to this extent does a disservice to both the authors (because it erroneously reflects poorly on the depth of their knowledge of the field) and the previous studies, so I encourage them to make a greater effort in referencing prior work. Some places where the lack of references particularly bothered me are called out in the specific comments below.***

A. We change the text about the reference. We include more references or put "e.g." in front of some citations.

## 2. Specific substantive comments and questions:

(1) ***L30: Liang et al. [2004], while not an inappropriate reference for the point that ASM air can be transported to distant locations, should certainly not be the ONLY paper cited for this point – in***

***fact, there are probably at least a dozen papers that could be added here.***

A. We include more references in the manuscript.

(2) ***L47-64: Although it is true that the NASM has received much less scientific attention than the ASM, it has not been neglected quite to the extent implied by these two paragraphs. I think that the authors should do a more thorough job of summarizing previous work on the influence of the NASM on UTLS composition. Given that water vapor is of particular interest in this manuscript, Anderson et al. [Science, 2012], Schwartz et al. [GRL, 2013], and Randel et al. [JGRA, 2015] should be mentioned. More generally, other references to consider including are: Q. Li et al. [JGR, 2005], Cooper et al. [JGR, 2006, 2007], Barth et al. [ACP, 2012], etc.***

A. More references are included in the manuscript, and the text is rephrased.

(3) ***Figure 1b: The 340 K surface seems too low to be appropriate for the map of MLS CO, which is not recommended for scientific use at pressures greater than 215 hPa. In fact, if proper data quality screening were applied, I would expect to see much of the tropics blanked out in a map of CO at this level. Thus some of the "hot spots" in this panel may be suspect. Since the specific level shown in this figure is not critical, I suggest 350 K instead.***

A. We agree the comment from the reviewer. We take the CO at 350 K in the revised version of the manuscript.

(4) ***L110-111: Some of the choices made here, while no doubt perfectly legitimate, should be explained. For instance, why are the simulations run over the 3-year period from 2010 to 2013? That is, why three years (and not two or ten), and why those particular years? Why are the tracers initialized over the interval 1 July through 31 August, when the anticyclone spins up by the beginning of June (if not earlier) and persists through September in most years? I am not suggesting that the analysis based on these choices is flawed, merely that they need to be better justified.***

A. We run the simulation at the same period as Ploeger et al. (2017) to have the direct comparison from different definitions of the domain boundary (simplified box and PV-barrier). We now added a sensitivity simulation where we set the artificial as 1 from 15 June to 15 September and run the simulation. Figure RL 1 shows the average air mass fraction from ASM and NASM regions initialized in the 350−360 K and 370−380 K layers during 15 June−15 September of 2010−2013 in the CLaMS-EI simulations during the following April−June. We can see a lot of similarities between Figure RL 1 and Fig.3 in the manuscript. Here, more monsoon tracer is transported into the stratosphere from the 350−360 K layer than from the 370−380 K layer for both the ASM and NASM regions. The abundance of monsoon air initialized at 350−360 K is higher in the SH stratosphere than in the NH, while monsoon air initialized at 370−380 K is more likely to remain in the NH. The monsoon air mass fraction in the stratosphere is higher than it from Fig.3 in the manuscript due to the longer simulation period here.

As Fig.8 in the manuscript, we also quantify the transport from source regions to the destination regions (Figure RL 2). The abundances of monsoon air in the three destination regions are larger than those from Fig.8 in the manuscript because of the longer simulation period. However, the transport patterns are quite similar. July and August is at the mature phase of the monsoon circulations. Using this period can transport less in-mixing of air from the adjacent regions of the monsoon regions. The simulation results from July and August include most of the features from longer period. The same

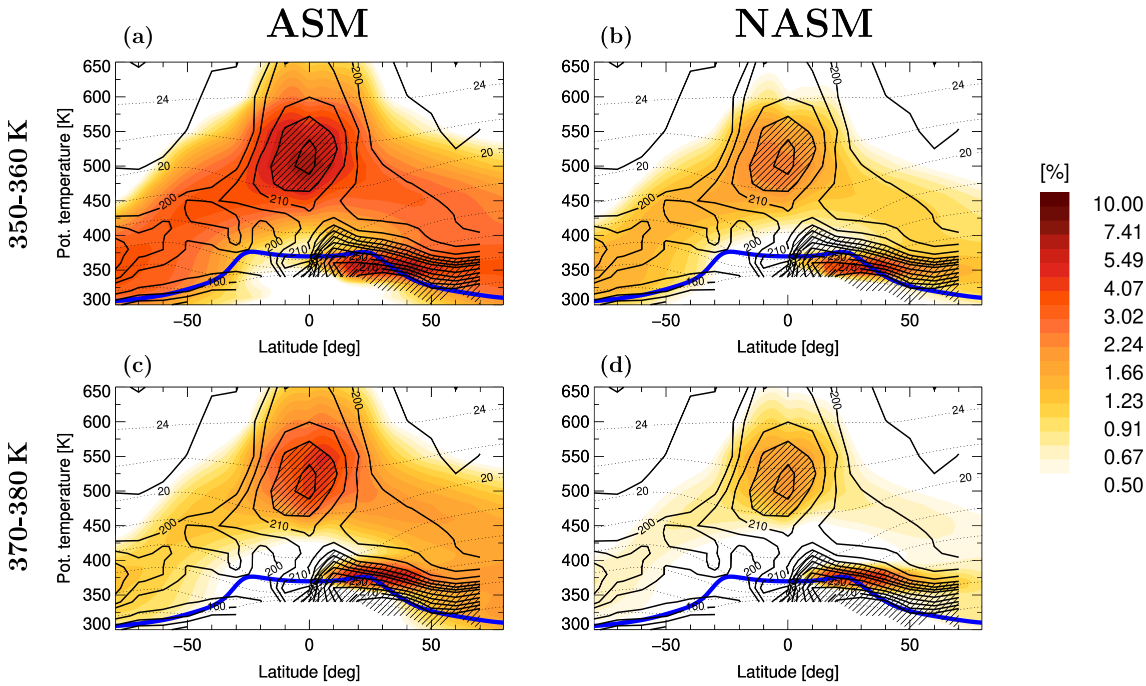


Figure RL 1: Climatological (2010−2013) zonal mean air mass fraction from the ASM (a and c) and the NASM (b and d) initialized at 350−360 K (upper) and 370−380 K (lower) in CLaMS-EI (color shading) during the following April−June. HCN from ACE-FTS observations (black contours) is also shown for context. Regions with HCN volume mixing ratios greater than 215 pptv are hatched. Blue lines mark the lapse rate tropopause. (Note the logarithmic color scale.)

range of simplified box domain of monsoon regions used in June and September may overestimate the contribution of transport from monsoon regions. The contributions of transport from ASM region to the TrP and LS-NH quantified in our work based on July-August period show similar values with the previous study covering the time period of May−October Vogel et al., 2019. Hence, we simulate the monsoon transport during July-August instead of June-September. We change the text and mainly include this point at the "Discussion" section of the manuscript.

(5) ***L110-111: L131: Similarly, why is the April-to-June period used for Figures 3 and 4? I assume that June was chosen as the end of the interval because the tracers are re-initialized at the start of the next ASM season in July. But why include results starting in April (and not March or May)?***

A. We would like to show the evolution of the monsoon tracers from July to June in the next year. The evolution process shows a lot of similarities with the results in Ploeger et al. (2017). To avoid the redundancy, we just show the result from April-June because it includes the transport to the tropical pipe which is import to the global stratosphere. We include the explanation in the revised version of the manuscript.

(6) ***L155-161: References should be given for all three of the effects listed in L157-158. I see why these factors would lead to higher column amounts in the SH at 350-360 K than in the SH at 370-380 K. But it is less clear to me why they would lead to higher column amounts in the SH at 350-360 K than in the NH at that level.***

A. The references are added in the manuscript. The higher column of monsoon air in the SH from 350-

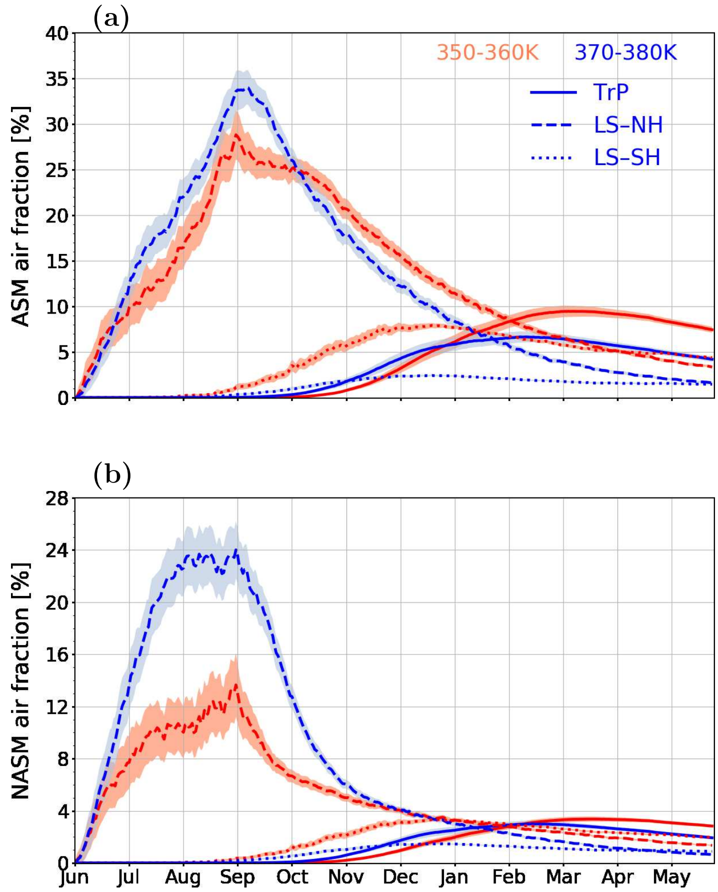


Figure RL 2: Climatological time series based on the CLaMS-EI simulations of source regions: (a) ASM and (b) NASM air mass fractions (in %) and diagnosed in three destination regions (see Fig.2 in the manuscript): tropical pipe (TrP, solid line), extratropical lower stratosphere in the NH (LS-NH, dashed line) and in the SH (LS-SH, dotted line). Shading shows the mean standard deviation in the zonal average (multiplied by 0.2 for better visibility). Red and blue lines respectively represent the tracers released in the 350−360 K and 370−380 K layer.

360 K is more connected to the seasonality of the Brewer-Dobson circulation. The monsoon tracers are compressed to the lower altitude with higher density in the SH compared to the monsoon tracers in the NH, this leads to the higher columns of the monsoon tracer in the NH at the end.

(7) ***L203-204: Other references would be appropriate here as well, including Bannister et al. [QJRMS, 2004], James et al. [GRL, 2008], and Dethof et al. [1999] (already cited elsewhere in the manuscript), etc.***

A. The references are added.

(8) ***L215: Again, a brief explanation of why the 400 K level is selected to be shown in Figure 6 might be good. Also, it might be helpful to add a horizontal line (maybe dashed or in grey) at this level in Figure 5, to orient the reader for the following plot.***

A. We choose 400 K to investigate the monsoon influence on the lowermost stratosphere. 380 K level is widely used to study the lowermost stratosphere, but it is too close to our source domain 370-380 K and may not represent the horizontal transport properly. The brief explanation is included in the manuscript. The grey dashed line is added in Fig.5.

(9) ***Figure 7: Have the results in this figure been aggregated over the 2010-2013 period? How was the particular interval shown (November-May) chosen? It would be good to define what is meant by "young" in the figure caption as well as the main text. As stated in L239-240, the tropical pathway is more common for tracers released at 350-360 K, but it does not appear to be entirely absent for the 370-380 K tracers in Figure 7c. There are hints of a "fork" in the ASM tracer distribution between ~3.7-4.0 ppmv and ~2% (in which case the cyan arrow may be slightly misplaced). There may even be a faint hint of similar structure for the NASM tracer (Figure 7d), but the cyan arrow, useful though it is, obscures it.***

A. The results in Fig.7 were based on 2010-2011. We didn't correlate the tracer and water vapor from the whole period because the annual variability makes the structure very obscure. We do check the results year by year, they all show similar structures. The text in the manuscript is changed, and a brief explanation is included. We choose the time period November-May considering the transit time (see also Ploeger et al., 2017 and Vogel et al., 2019) from monsoon regions to the tropical pipe. The definition of "young" air mass is included in the caption as well. We agree the tropical pathway is not totally absent for 370-380 K. Although the air in 370-380 K layer over monsoon regions is less leaky than the air in 350-360 K, there is still the possibility of horizontal transport through tropics. This point is added in the revised version of the manuscript.

(10) ***L262-263: Is this time difference consistent with known upwelling rates? (A reference would be good.)***

A. The upwelling rate is about 10-20 days/10 K. The references are added in the draft.

(11) ***Figure 8: I understand that scaling the standard deviations improves the legibility of the plot, but multiplying by 0.2 seems like a fairly drastic step that produces a misleading impression of the degree of variability. How can such a substantial reduction in the scatter in this plot be justified? If the full envelopes were presented, results for the various destination regions would likely overlap significantly. As it is, I fear that the figure instills more confidence in the separability of the regions than is really warranted.***

A. We agree the scale of 0.2 is too small. Indeed, the results are substantially overlapped if we plot the original standard deviation. It is difficult to see the structures. In the revised manuscript, we multiply the standard deviation by 0.5. We can see the overlap results and the mean time series clearly.

(12) ***L314-318: To my eye, the TE into the LS-SH is never dominated by ASM or NASM sources for tracers released at 370-380 K – after February, the curves for all three sources lay nearly on top of one another. Moreover, for the ASM tracers transport from the 350-360 K layer dominates over that from the Tropics starting in December, not January. Finally, the TE from the ASM is nearly 50% larger than that from the NASM, so perhaps "slightly" should be deleted in L318.***

A. We made a mistake to calculate the air mass of the tropical source domain, it affected the calculation of the transport efficiency from tropics, especially for the tropical source tracer released at 370-380 K. We combined the comments from the reviewer and rephrased the paragraph. "The ASM tracers transport from the 350-360 K layer dominates over that from the Tropics starting in December." is changed in the text. The result related to "slightly" is removed.

(13) ***L340-341: It would be appropriate to include here some references for the effects of Rossby wave***

***breaking and eddy shedding on mixing monsoon air into the extratropics.***

A. Several references regarding this point are added.

(14) ***L404-411: I was confused the first couple of times that I read this paragraph, because I expected the results cited here to have been shown in Figure 11 - it is the last figure in the paper and freshest in readers' minds when they arrive at the Conclusions. I hadn't understood what was meant by "ultimate" in L404 (in fact, I don't think that the usage of that word conveys quite what the authors intend), and so it took me several minutes to realize that the numbers being quoted here for the most part refer to the end of the simulation period in Figures 8 or 9 and thus do not match the values in Figure 11. I concede that I obviously was not reading these sentences carefully enough, but I'm guessing that many readers may do the same and also may fail to note that Figure 11 shows the "maximum" contributions/efficiencies. That information is noted in the figure caption, but it is not stated when this figure is introduced in L358, which instead describes it as showing "overall contributions, efficiencies, and transit times". In addition, stating values such as 0.9 for the TE in L410 without specifying that this value refers to the end of the simulation compounds the confusion, as does stating a range for the TE from the Tropics to the TrP. In my mind this entire discussion needs to be clarified, with a bit more hand-holding to help the reader follow the details. However, this brings up a philosophical question about whether showing the maximum contributions/efficiencies is really the best approach for Figure 11. Moreover, while reading this paragraph I also wondered why a similar panel for the Tropics was not included in that figure.***

A. We explain the meaning of "ultimate" time in the text. We think that the maximum and ultimate contribution and efficiency of transport from the source regions to the destination regions may help to explain the transport of pollutants with different lifetime to the stratosphere. For better comparison, we summarize the results of the transport from three source regions (ASM, NASM, and Tropics) to three destination regions (LS-NH, LS-SH, and TrP) at the end of the draft.

# 3. Minor points of clarification, wording suggestions, and grammar / typo corrections:

(1) ***L30: influences –> influence***

A. The text is changed.

(2) ***Figure 1 caption: I questioned the need for the seemingly unimportant detail about the map being produced by python in my initial access review, and I still don't see why this information is useful to the reader. A similar comment applies to Figure. 10.***

A. The sentence about the map information in Fig.1 and Fig.10 is removed.

(3) ***L57: "Meanwhile" seems like an odd choice of word here***

A. The sentence is changed.

(4) ***L93: add a comma after "anticyclone"***

A. A comma is included.

(5) ***L116: TrP has already been defined (L41)***

A. We write the full term Tropical pipe (TrP) together with the extratropical lowermost stratosphere in the Southern Hemisphere (LS-SH) and the extratropical lowermost stratosphere in the Northern

Hemisphere (LS-NH) to make the definition of the destination regions more clear. To avoid repetitive definition, we remove the first TrP in the introduction.

(6) ***Figure 3 and caption. Although it is stated in the main text, it would be good to add "in July and August" somewhere in the caption, perhaps after "initialized" or before "in CLaMS-E1". Also, some odd glitches are apparent in the dashed line in this figure, especially in panel 3b at about (45N, 10m).***

A. The simulation period " in July and August" is added in the caption of Fig.3, the figures are also changed.

(7) ***L155: The interhemispheric difference is fairly small, especially for the total column, so I suggest adding "slightly" in front of "larger"***

A. "slightly" is added in front of "larger".

(8) ***L156: since this sentence is about the SH, just to be really clear, add "boreal" in front of "monsoon"***

A. "boreal" is added in front of "monsoon".

(9) ***L158-159: portion . . . enters . . . and is (not "enter" and "are")***

A. The text is changed.

(10) ***L173: add a comma after "simulations"***

A. A comma is added after "simulations".

(11) ***L177: "not shown" – is this point not shown by comparison of Figures 3 and 4?***

A. We can see this point by the comparison of Fig.3 and Fig.4. We write "not shown" because we did not include the figure about the inter-hemisphere difference directly. We remove "not shown" in the revised version of the draft.

(12) ***Figure 5 caption: I think it would be helpful to add "over the July 2010 to April 2014 period" after "sections".***

A. "during July 2010 to June 2014" is added in the caption of Fig.5.

(13) ***L210:. . . tracers is slightly lower –> . . . tracers is slightly weaker***

A. The text is changed.

(14) ***L221: "spread out" might be better than "widespread"***

A. Thank you for the suggestion. We choose "widespread" to emphasize the wider transport in CLaMS-M2 compared to CLaMS-EI.

(15) ***L239: ASM (NASM) –> ASM (NASM) region***

A. "region" is added.

(16) ***L255: show –> shows***

A. The text is changed.

(17) ***L264-266: it would draw the contrast (and flow) better to move "after three months" to right after "However," at the beginning of the sentence.***

A. The sentence is rephrased.

(18) ***Figure 8 caption: I think it might work better to say ". . . simulations of air mass fractions (in %) in three source regions"***

A. The caption is changed as suggested.

(19) ***L268: that –> those***

A. The text is changed.

(20) ***L271: it might be good to add "throughout the year" at the end of this sentence***

A. "throughout the year" is added at the end of the sentence.

(21) ***L279-280: it might be good to add "As for the ASM," at the beginning of this sentence***

A. "As for the ASM," is added at the beginning of the sentence.

(22) ***L289: it might be good to add "Much" in front of "more air"***

A. "Much" is added in front of "more air".

(23) ***L291: delete "and"***

A. "and" is deleted.

(24) ***L297: delete "up to and"***

A. "up to and" is deleted.

(25) ***L321: To me, "after March" means "starting in April", but in fact the NASM TE exceeds the tropical TE in the TrP region at the beginning of March for the 350-360 K tracers. Thus "after March" should be "by March". Similarly, "after April" should be "by April". In addition, there is a typo at the end of this line: 380 KIn –> 380 K. In***

A. The text is changed to "by March". Because of the mistake about calculating the mass of tropical domain, the results were rephrased here. The typo is corrected.

(26) ***L325-326: that –> those. Also, the CLaMS-M2 figure is omitted so I cannot judge myself, but I assume that a similar issue to the point raised above exists for "after December . . . or January".***

A. The text is changed. The point about "after December . . . or January" is checked and revised.

(27) ***L337-339: these two sentences are somewhat redundant and could be combined for efficiency (and to eliminate the slightly awkward construction ". . . Fig. 10. Figure 10 . . ."). Also, when were the results for 24 August 2012 shown in this figure initialized?***

A. The two sentences are rephrased and combined to one sentence. The results on 24 August 2012 are based on the tracers initialized from 1 July 2012 to 24 August 2012.

(28) ***L342-343: replace the second instance of "CLaMS-EI and CLaMS-M2" in this line with "the two simulations"***

A. The text is changed.

(29) ***L366: it would be good to remind readers of these pathways by adding "(monsoon and tropical)" after "pathways"***

A. "(monsoon and tropical)" is included in the after "pathways".

(30) ***L371: It is very confusing to start this sentence with "As for the NASM". This kind of construction is often used to set up a discussion of similarity, but the previous sentence is also talking about the NASM, so that doesn't make sense. You may have meant "As is the case for the ASM", in which***

***case there is a typo ("NASM" should be "ASM"). That's what I assumed the first time I read this sentence, so I suggested making that change in my access review. Since the phrase remains in this version, I am guessing that was not your intention, and thus it is probably best to simply delete this phrase.***

A. I didn't understand your access review correctly. It is a typo here. We remove this sentence to make the point less confusing in the revised manuscript.

(31) ***L375: maybe add "(not shown)" again at the end of the sentence***

A. "(not shown)" is added at the of the sentence.

(32) ***L386: I feel that the Conclusions section starts too abruptly – it needs some sort of introductory sentence to set the stage and sum up what was done in the paper. On the other hand, such a sentence is not really needed at the beginning of the Discussion section. Thus I suggest moving the first sentence in that section ("We have investigated. . .", L330-331) here.***

A. The paragraph about the beginning of "Discussion" and "Conclusions" are changed as suggested.

(33) ***L389-390: "vertical differences" is awkward. I suggest instead "differences in the dynamical situation with altitude"***

A. The text is changed as suggested.

(34) ***References: the doi's for many of the references are repeated.***

A. The "References" are checked and corrected.

# Referee3

Many thanks to the reviewer for the comments, and they have helped to improve the clarity of the manuscript. In the following, we address all the points raised in the review (denoted by italic letters). Text changes in the manuscript are highlighted in red or blue.

## *General comments*

***Overall this is an important and well written paper that will be a serious contribution to the literature about the role of the monsoon transport in the UTLS region. I really liked the idea that there are two pathways and that the model statistics support those pathways.***

1. ***I think it would be helpful to summarize the efficiencies of the pathways and the differences in the models in a Table instead of text. Also Figure 11 should have the efficiency of the UT pathway to the base of the tropical pipe. The authors might also connect the efficiency of transport to the containment in the monsoons (see Pan et al, 2016, Transport of chemical tracers from the boundary layer to stratosphere associated with the dynamics of the Asian summer monsoon, J. Geophys. Res. Atmos., 121, 14,159−14,174, doi:10.1002/2016JD025616.) who showed that the ASM is not as leaky as the NASM.***

   A. We summarize the contribution and efficiency of transport and transit time from the source regions to the destination regions in the end of the manuscript. The numbers in red color in Fig.11 represent the sum of transport along monsoon and tropical pathways from 350−360 K over monsoon regions to the tropical pipe. The separation of the contribution of transport along different pathways to the tropical pipe is included in the discussion section with more than 50% of contributions from tropical pathway. Regarding the last point, we didn't find the work about NASM from Pan et al., 2016. We include two more subplots from MLS CO in the revised manuscript. Indeed, the ASM is not as leaky as the NASM. We also connected this point to the transport to the LS-NH in Section 4.

2. ***My major problem with this paper is I really don't understand the percentage argumentn used by the authors. Page 5 line 110 on the model set up confuses me. If I understand what the authors are doing is that they are starting up the model with some kind of uniform grid of parcels inside monsoon domain and the tropics. The model is running forward trajectories and then estimating the tracer ends up in each region. But as the system evolves, air from the SH will enter the tropics and air outside the monsoons will enter the monsoon region. The authors don't say how they account for this outside air in the estimates of the percentages after August 1. To be clear, I am not saying that the authors have done this wrong, but this paragraph gives me the impression that the CLaMS parcels are initiated over a limited domain. If this is true then it seems like the percentage estimates will be incorrect.***

   A. The text was not so clear about the setup of the model. The tracer set-up is the same as in Orbe et al. (2015), Ploeger et al. (2017). We set the artificial tracer mixing ratio as 1 inside the monsoon regions and the tropics during July and August. The model simulations are driven by horizontal winds and diabatic heating from reanalysis. We estimate the abundance of source tracer at any location in the atmosphere. The percentage in our study represents the monsoon/tropical tracer mixing ratio at any location, and it equals the fraction of air which left the corresponding source layer in the ASM, NASM or tropical domain during the previous monsoon season. The transport from different source regions is simulated independently in our study. Therefore, there is no interactive influence among the transport from the three source regions. Based on the comment, we rephrase the text in the manuscript to make it more clear.

3. ***A second issue is that the authors initialize on July 1 of each year assuming that the monsoon develops about that time and then they stop tagging parcels after August 1. This seems like a limitation since the monsoon circulation can persist through early September. It seems to me some additional runs of the model would put to rest the sensitivity of their results to the limited tagging period.***

   A. We run the simulation for the same period as Ploeger et al. (2017) to have the direct comparison from different definitions of the domain boundary (simplified box and PV-barrier). As suggested by the Reviewer, we now added a sensitivity simulation where we set the artificial tracer as 1 from 15 June to 15 September and run the simulation. Figure RL 1 shows the average air mass fraction from ASM and NASM regions

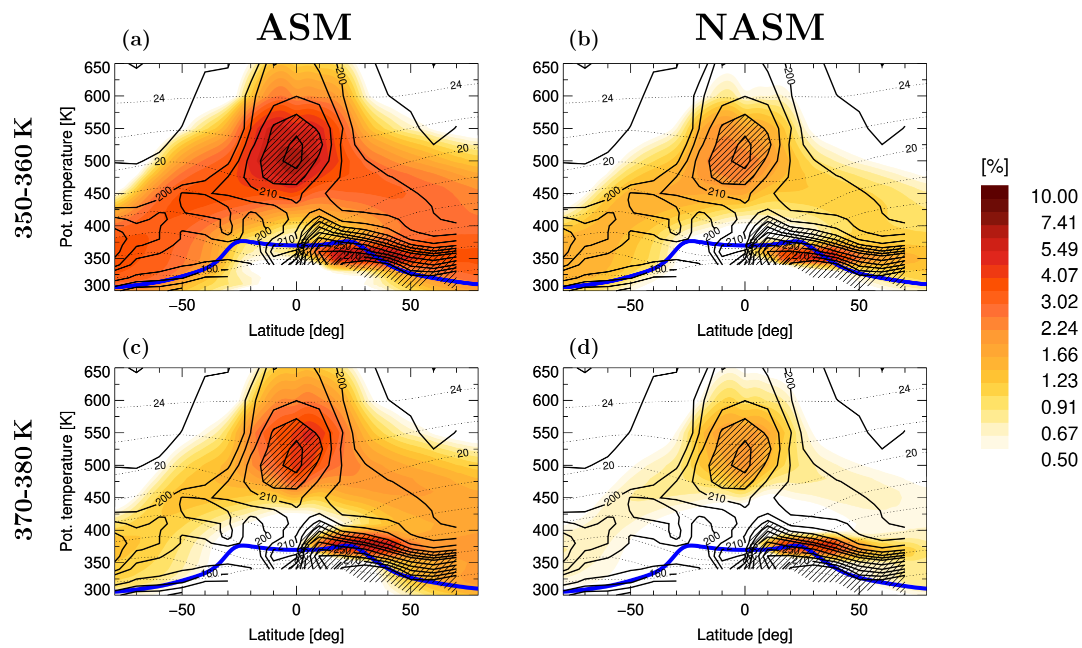


Figure RL 1: Climatological (2010−2013) zonal mean air mass fraction from the ASM (a and c) and the NASM (b and d) initialized at 350−360 K (upper) and 370−380 K (lower) in CLaMS-EI (color shading) during the following April−June. HCN from ACE-FTS observations (black contours) is also shown for context. Regions with HCN volume mixing ratios greater than 215 pptv are hatched. Blue lines mark the lapse rate tropopause. (Note the logarithmic color scale.)

   initialized in the 350−360 K and 370−380 K layers during 15 June−15 September of 2010−2013 in the CLaMS-EI simulations during the following April−June. We can see a lot of similarities between Figure RL 1 and Fig.3 in the manuscript. In particular the transport patterns are not depending on the exact length of the initialization period. More monsoon tracer is transported into the stratosphere from the 350−360 K layer than from the 370−380 K layer for both the ASM and NASM regions. The abundance of monsoon air initialized at 350−360 K is higher in the SH stratosphere than in the NH, while monsoon air initialized at 370−380 K is more likely to remain in the NH. The exact value of monsoon air mass fraction in the stratosphere is higher for the the longer initialization period.

As Fig.8 in the manuscript, we also quantify the transport from source regions to the destination regions

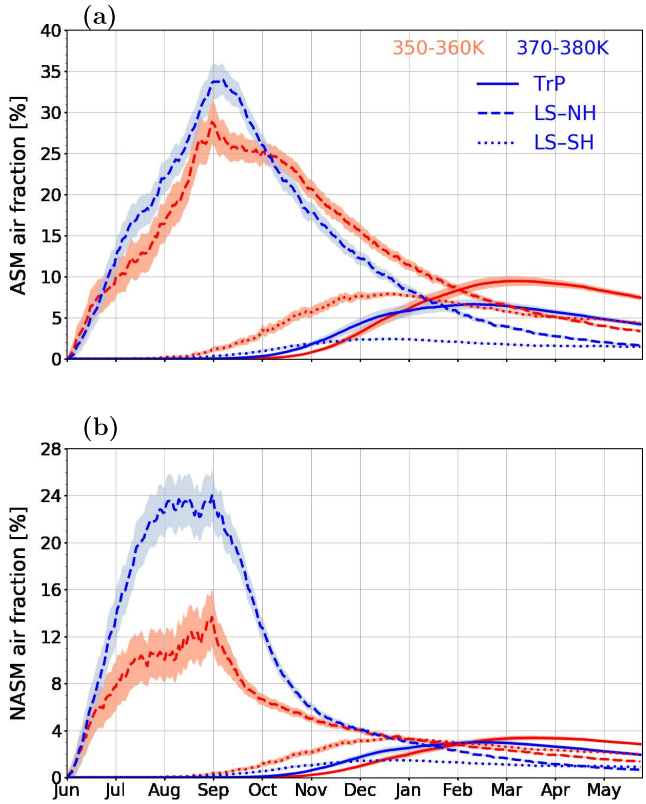


Figure RL 2: Climatological time series based on the CLaMS-EI simulations of source regions: (a) ASM and (b) NASM air mass fractions (in %) and diagnosed in three destination regions (see Fig.2 in the manuscript): tropical pipe (TrP, solid line), extratropical lower stratosphere in the NH (LS-NH, dashed line) and in the SH (LS-SH, dotted line). Shading shows the mean standard deviation in the zonal average (multiplied by 0.2 for better visibility). Red and blue lines respectively represent the tracers released in the 350−360 K and 370−380 K layer.

(Figure RL 2). The abundances of monsoon air in the three destination regions are larger than those from Fig.8 in the manuscript because of the longer simulation period. However, the transport patterns are quite similar. July and August is at the mature phase of the monsoon circulations. Using this period can transport less in-mixing of air from the adjacent regions of the monsoon regions. The simulation results from July and August include most of the features from longer period. The same range of simplified box domain of monsoon regions used in June and September may overestimate the contribution of transport from monsoon regions. The contributions of transport from ASM region to the TrP and LS-NH quantified in our work based on July-August period show similar values with the previous study covering the time period of May−October Vogel et al., 2019. Hence, we simulate the monsoon transport during July-August instead of June-September. We added a remark on this sensitivity in the discussion section of revised manuscript (P22).

4. ***Clearly Page 5 needs a lot of clarification. Since all of the rest of the paper is a function on how CLaMS was used here, I suggest the authors spend a little more time on the model set up and the assumptions***

***behind it.***

A. Thanks for pointing this out. More details about model setup and assumptions are included in the revised version of the draft.

5. ***Minor comments: You don't need to tell us you used Python to make a figure.***

   A. The information about Python is removed.

# The efficiency of transport into the stratosphere via the Asian and North American summer monsoon circulations

Xiaolu Yan[1], Paul Konopka[1], Felix Ploeger[1], Aurélien Podglajen[1], Jonathon S. Wright[2], Rolf Müller[1], and Martin Riese[1]

[1]Forschungszentrum Jülich (IEK-7: Stratosphere), Jülich, Germany
[2]Department of Earth System Science, Tsinghua University, Beijing, China

**Correspondence:** Xiaolu Yan (x.yan@fz-juelich.de)

**Abstract.** Transport of pollutants into the stratosphere via the Asian summer monsoon (ASM) or North American summer monsoon (NASM) may affect the atmospheric composition and climate both locally and globally. We identify and study the robust characteristics of transport from the ASM and NASM regions to the stratosphere using the Lagrangian chemistry transport model CLaMS ~~as driven by~~ driven by both the ERA-Interim and MERRA-2 reanalyses. In particular, we ~~investigate~~ quantify the relative influences of the ASM and NASM on stratospheric composition ~~,~~ and investigate the transport pathways ~~by which these influences are effected, and the quantitative contributions~~ and efficiencies of transport ~~from~~ of air masses originating at different altitudes in these two monsoon regions to the stratosphere. We release artificial tracers in several vertical layers from the middle troposphere to the lower stratosphere in both ASM and NASM source regions during July and August 2010−2013 and track their evolution until the following summer. We find that ~~the magnitude of transport~~ more air mass is transported from the ASM and NASM regions to the tropical stratosphere, and even to the Southern Hemispheric stratosphere, ~~is higher~~ when the tracers are released ~~at the~~ clearly below the tropopause (350−360 K~~level~~) than when they are released close to the tropopause (370−380 K). For tracers released close to the tropopause (370−380 K), transport is primarily into the Northern Hemispheric lower stratosphere. Results for different vertical layers ~~or~~ of air origin reveal two transport pathways from the upper troposphere over the ASM and NASM regions to the tropical pipe: (i) quasi-horizontal transport to the tropics below the tropopause followed by ascent to the stratosphere via tropical upwelling, and (ii) ascent into the stratosphere inside the ASM/NASM followed by quasi-horizontal transport to the tropical lower stratosphere and further to the tropical pipe. ~~The~~ Overall, the tropical pathway (i) is faster than the monsoon pathway (ii), particularly in the ascending branch. ~~Ultimately, the~~ The abundance of air in the tropical pipe that originates in the ASM upper troposphere (350−360 K~~, ∼5%~~) is comparable to ~~that~~ the abundance of air ascending directly from the tropics to the tropical pipe ten months after (the following early summer) the release of the source tracers. ~~By contrast, the~~ The air mass contributions from the ASM to the tropical pipe are about three times larger than the corresponding ~~contribution~~ contributions from the NASM~~(∼1.5%)~~. The transport efficiency into the tropical pipe, the air mass fraction inside this destination region normalized by the mass of the domain of origin, is greatest from the ASM region at 370−380 K. ~~Transport from the ASM to the tropical pipe is almost twice as efficient as transport from the NASM or tropics to the tropical pipe.~~ Although the contribution from the NASM to the stratosphere is less than that from either the ASM or the tropics, the transport efficiency from the NASM is comparable to that from the tropics.

## 1 Introduction

The structure and composition of the upper troposphere and lower stratosphere (UTLS) during boreal summer and fall over Asia and North America have many unique features. The Asian summer monsoon (ASM) and North American summer monsoon (NASM) anticyclones are not only important locally, but also affect first the entire northern hemisphere (NH) and then the whole atmosphere ~~(Vogel et al., 2016; Ploeger et al., 2017; Yu et al., 2017; Vogel et al., 2019)~~(e.g. Dethof et al., 1999; Randel et al., 2010, 2012; . These circulations ~~pump vast~~ transport large amounts of water vapor and other chemical constituents from the surface to the UTLS ~~(?Randel et al., 2010)~~(e.g. Rosenlof et al., 1997; Li et al., 2005; Park et al., 2009; Chirkov et al., 2016; Santee et al., 2017; Rolf et a . Air originating in the ASM and NASM is lifted high enough to ascend ~~freely~~ into the stratosphere and can be transported to distant locations ~~(?)~~(e.g. Vogel et al., 2016; Fadnavis et al., 2018), where it may exert considerable ~~influences on stratospheric chemistry , radiation and dynamics (Vogel et al., 2016)~~influence on UTLS chemistry (e.g. Cooper et al., 2006; Barth et al., 2012; Gottschal and the radiative forcing of surface temperature (e.g. Solomon et al., 2010; Riese et al., 2012; Roy, 2018). Hence, transport of air uplifted by the ASM and NASM is an important factor influencing the composition of the UTLS and the evolution of global climate.

Transport via the ASM ~~has drawn extensive attention. This transport~~ involves deep convection uplifting air from the boundary layer to the UTLS ~~(Fu et al., 2006; Randel et al., 2010; Wright et al., 2011; Bergman et al., 2012; Fadnavis et al., 2015; Santee et al., 2017~~ (e.g. Randel and Park, 2006; Wright et al., 2011; Bergman et al., 2012; Tissier and Legras, 2016), including the injection of boundary layer air by typhoons over Southeast Asia and Western Pacific into the outer regions of the ASM anticyclone ~~(Vogel et al., 2014; Li et al.~~ (Vogel et al., 2014; Li et al., 2018). At higher levels, transport is dominated by the strong ASM anticyclone ~~(Randel and Park, 2006; Park et~~ (e.g. Randel and Park, 2006; Park et al., 2008; Vogel et al., 2019), which is confined by easterly (on the tropical side) and westerly (on the extratropical side) jets. These jets act as strong transport barriers and restrict isentropic mixing ~~(?Poshyvailo et al., 2018)~~ (e.g. Ploeger et al., 2015; Poshyvailo et al., 2018). High concentrations of tropospheric tracers and low concentrations of stratospheric tracers within the anticyclone are evident in a variety of observations ~~(Park et al., 2008; Randel et al., 2010; Vogel et al., 2014; Unge~~ (e.g. Park et al., 2008; Glatthor et al., 2015; Ungermann et al., 2016; Santee et al., 2017; Höpfner et al., 2019). A fraction of the air within the ASM anticyclone eventually enters the tropical pipe ~~(TrP)~~ and the NH extratropical lowermost stratosphere like a vertical 'chimney' ~~and~~ or an isentropic 'blower' (Pan et al., 2016; Ploeger et al., 2017). The processes involved in this transport affect the chemical composition of the UTLS, including the buildup of ozone precursors ~~(Fadnavis et al., 2015) and the~~ (e.g. Fadnavis et al., 2015) and the formation of the Asian tropopause aerosol layer (ATAL) (Vernier et al., 2011; Yu et al., 2017; Vernier et al., 2018; Brunamonti et al., 2018). ~~The latter~~ Recently, it has been suggested that a significant fraction of ATAL particles are composed of ammonium nitrate with ammonia from ground sources being the precursor pollutant (Höpfner et al., 2019). The ATAL has been estimated to cause a significant regional radiative cooling of the Earth's surface with an intensity of $\sim$0.1 W m$^{-2}$ ~~(Vernier et al., 2011, 2015)~~(Vernier et al., 2015).

In comparison to the ASM, transport to the stratosphere via the NASM has received relatively little scientific attention~~to date~~. Chen (1995) found that significant stratosphere-troposphere exchange (STE) occurs at potential ~~temperature~~ temperatures greater than 340 K in the NH during boreal summer and linked this exchange ~~with~~ to the ASM and NASM circulations.

Dunkerton (1995) reported that the influence of monsoon circulations on STE vanishes above ∼25 km. Water vapor retrievals from the Halogen Occultation Experiment (HALOE) satellite revealed two pronounced maxima over Asia and North America, presumably related to monsoon-driven convection over these two regions (Dethof et al., 1999; Randel et al., 2001). Dessler and Sherwood (2004) pointed out that summer convection over North America is sufficient to exert a significant effect on the water vapor budget in the extratropical lower stratosphere, although not on the ozone budget. However, Randel et al. (2015) found that stratospheric water vapor in the ASM and NASM regions is mainly controlled by large-scale circulation and temperatures instead of overshooting deep convection. Gettelman et al. (2004) argued that the NASM may entrain air from the high latitude troposphere into the subtropical lower stratosphere, but this air would rarely reach the deep tropics. ~~However, using~~ Using satellite observations, Randel et al. (2012) linked a positive anomaly in the deuterium content of lower stratospheric water vapor to the NASM (and not the ASM) and showed that this anomaly extends into the tropics. ~~Meanwhile~~The injection of water vapor into the stratosphere over the NASM may change the catalytic chlorine/bromine free-radical chemistry which could have implications for ozone loss (Anderson et al., 2012; Robrecht et al., 2019; Clapp and Anderson, 2019); however, Schwartz et al. (2013) found no indication of substantial ozone depletion triggered by injection of water vapor over the NASM region based on MLS data. Although water vapor in the stratosphere is strongly affected by the NASM, model simulations driven by the ERA-Interim reanalysis ~~products~~ suggest that the fraction of NASM air in ~~NH midlatitudes~~ the NH midlatitude lower stratosphere is about one order of magnitude smaller than the fraction of ASM air (Ploeger et al., 2013).

Figure 1a shows ~~clear anticyclonic circulations associated with higher tropopause levels~~ higher tropopause altitudes over the ASM and NASM regions associated with anticyclonic circulations during July−August based on both the ERA-Interim and MERRA-2 reanalyses. Correspondingly, measurements of CO from the Aura Microwave Limb Sounder (MLS) show high values at ~~340~~350 K over the ASM and NASM regions (Fig. 1b). Potential temperature−latitude sections of CO across the ASM (90° E, Fig. 1c) and NASM (90° W, Fig. 1d) anticyclones show that the enhancement of CO extends up to the UTLS with strong confinement over the ASM region and weak confinement over the NASM region. As described above, most previous studies have focused on the transport pathways related to the ASM anticyclone, with relatively few ~~contributions related to the~~ analyses of transport via the NASM anticyclone. In this study, we address the following questions:

(1) How does transport from the ASM and NASM regions affect stratospheric composition?

(2) How large are contributions from the ASM and NASM regions to the stratosphere relative to contributions from the inner tropics?

(3) From which levels within the ASM and NASM regions do the most effective transport pathways to the stratosphere originate?

Studies of air mass transport across the tropopause often rely on winds and diabatic heating rates from reanalyses. Diabatic heating rates, especially if derived from reanalyses, are more suitable to quantify vertical transport than ~~the~~ are pressure tendencies, which are strongly affected by the numerical noise of the assimilation procedure (Eluszkiewicz et al., 2000; Schoeberl et al., 2003). However, diabatic heating rates are highly uncertain ~~,~~ and differ substantially among reanalyses (Randel and Jensen, 2013; Wright and Fueglistaler, 2013; Abalos et al., 2015). These differences have important implications for transport calculations in the UTLS (Wright et al., 2011; Schoeberl et al., 2012; Bergman et al., 2013; Wang et al., 2014; Abalos et al., 2015;

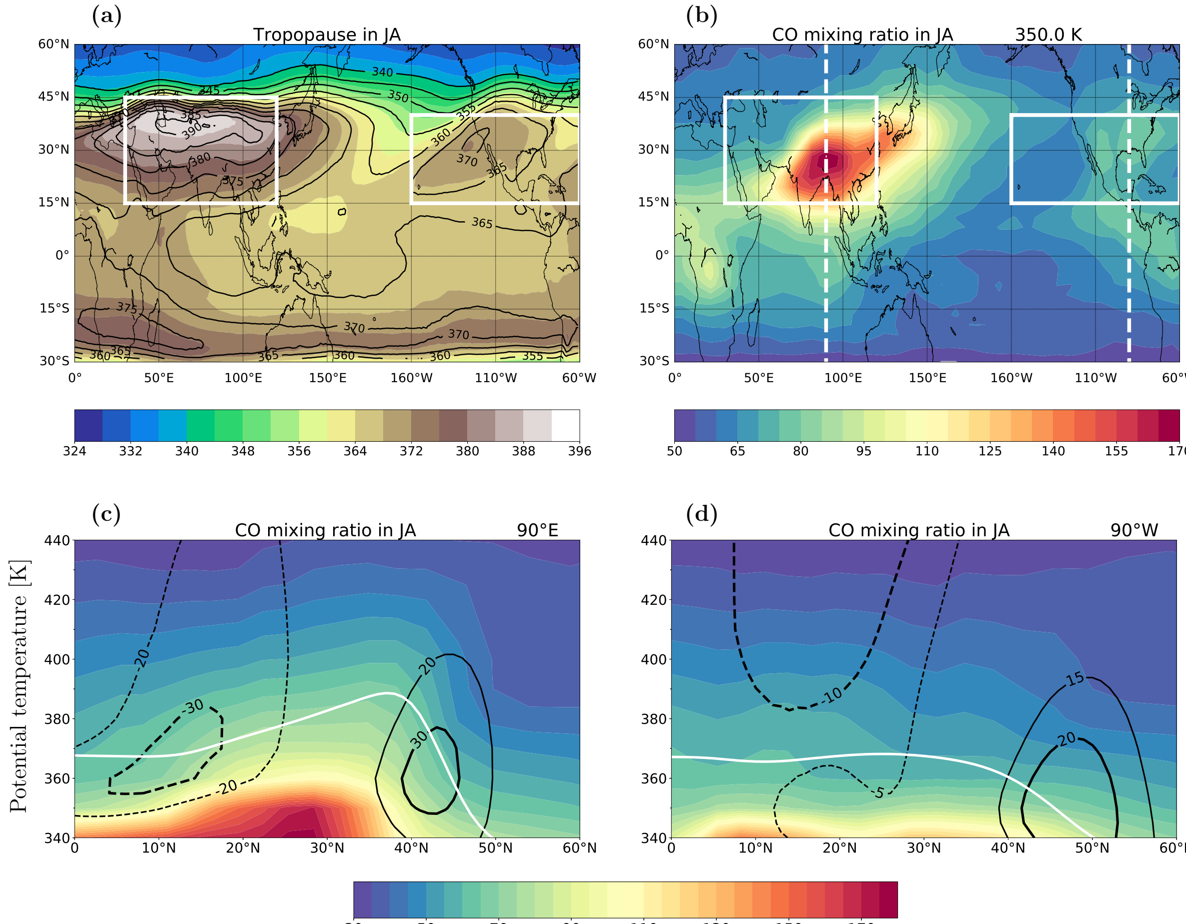


**Figure 1.** (a): Climatologies of the tropopause (lapse rate) potential temperature (in K) from ERA-Interim (1979−2016, color shading) and MERRA-2 (1980−2016, contours) for July and August. (b): Climatologies of CO (in ppbv) at $\theta$=~~340~~350 K calculated from MLS (2004−2016) for July and August. ~~Map is created by python~~(c,d): Potential temperature−latitude sections of CO (in ppbv, color shading) from MLS, tropopause height (white line) and wind (in m/s, black contours) from ERA-Interim for July and August during 2004−2016 along 90° E (c) and 90° W (d).

Ploeger et al., 2019; Tao et al., 2019). To evaluate the robust characteristics of transport in different reanalyses, we use both the ERA-Interim and MERRA-2 reanalyses to drive the Lagrangian transport model CLaMS. We then investigate the pathways for air mass transport from the ASM and NASM anticyclone into the lower stratosphere and quantify the associated transport efficiencies ~~(TE) and the amounts~~ and fractions of stratospheric air originating from each source region using both sets of simulations. In Sect. 3, we discuss reanalysis-related differences in the statistics of transport from monsoon regions to the extratropical lower stratosphere and ~~TrP~~ the tropical pipe, and investigate the influences of the ASM and NASM on stratospheric composition (e.g. HCN~~and~~, water vapor). In Sect. 4, we assess the efficiency of transport to the stratosphere via the ASM and NASM anticyclones. We discuss our findings in Sect. 5 before closing with a brief summary of the key results.

## 2 Data and methods

We apply tracer-independent diagnostics (i.e. without chemistry and emissions) to quantify air mass transport through the ASM anticyclone, NASM anticyclone and tropics. All diagnostics are based on simulations using the Lagrangian chemistry transport model CLaMS (McKenna et al., 2002; Konopka et al., 2004; Pommrich et al., 2014). The model transport is driven by horizontal winds and total diabatic heating rates from either the ERA-Interim (CLaMS-EI) or MERRA-2 (CLaMS-M2) reanalysis (for more details see Ploeger et al. 2019 or Tao et al. 2019). The use of two reanalysis data sets provides important constraints on the range of possible outcomes and potential biases associated with differences in horizontal winds and total diabatic heating rates between these two reanalyses.

We include artificial air mass origin ~~tracers in the model~~ fractions (AOFs; see also Orbe et al. 2013; Ploeger et al. 2017) to diagnose the fraction of air at any location in the stratosphere which left either ~~of the monsoon anticyclones~~ the monsoon regions or the tropics during the previous boreal summer monsoon season. There are several ways to define the ASM anticyclone, including Montgomery stream function (Santee et al., 2017), stream function (Yan et al., 2018; Tweedy et al., 2018), geopotential height (Pan et al., 2016) and potential vorticity (PV; Ploeger et al., 2017). Applying similar criteria to the NASM is less straightforward.

Here, we follow the geographic definition of the ASM source region proposed by Yu et al. (2017), which covers the domain [15° N, 45° N, 30° E, 120° E]. Within this region, we consider several different layers~~that~~, which collectively cover the atmospheric column from the middle ~~troposphere to the UTLS~~to upper troposphere. For the layer spanning $370-380$ K potential temperature, our results are very similar to those of Ploeger et al. (2017), who used a PV-based approach to define the anticyclone (detailed comparisons are provided below). We therefore ~~elect~~ decide to use this simple geographical domain to represent the ASM region. One of the motivations for this approach is that it ~~offers direct analogues~~ can be simply applied for the NASM region [15° N, 40° N, 160° W, 60° W] and the tropics [15° S, 15° N] ~~. Note that the use of either a regular box or a PV contour to define the ASM region yields very similar results, as shown by Garny and Randel (2016)~~as well. Vertically, we divide the column of air from the middle troposphere to the lower stratosphere above each region into 4 potential temperature layers $340-350$ K, $350-360$ K, $360-370$ K and $370-380$ K with $i$ labeling the layer.

$$M^i_{\mathrm{ASM}}(\lambda,\phi,\theta,t) = \begin{cases} 1 & \lambda \in [30^\circ\,\mathrm{E}, 120^\circ\,\mathrm{E}],\ \phi \in [15^\circ\,\mathrm{N}, 45^\circ\,\mathrm{N}],\ \theta \in \mathrm{Box}_i, \text{ and t} \in [\text{July, August}] \\ 0 & \text{elsewhere} \end{cases}$$

$$M^i_{\mathrm{NASM}}(\lambda,\phi,\theta,t) = \begin{cases} 1 & \lambda \in [160^\circ\,\mathrm{W}, 60^\circ\,\mathrm{W}],\ \phi \in [15^\circ\,\mathrm{N}, 40^\circ\,\mathrm{N}],\ \theta \in \mathrm{Box}_i, \text{ and t} \in [\text{July, August}] \\ 0 & \text{elsewhere} \end{cases}$$

$$M^i_{\mathrm{Tropics}}(\lambda,\phi,\theta,t) = \begin{cases} 1 & \lambda \in [180^\circ\,\mathrm{W}, 180^\circ\,\mathrm{E}],\ \phi \in [15^\circ\,\mathrm{S}, 15^\circ\,\mathrm{N}],\ \theta \in \mathrm{Box}_i, \text{ and t} \in [\text{July, August}] \\ 0 & \text{elsewhere} \end{cases}$$

Here $M^i_{\mathrm{ASM}}$~~$(\lambda,\phi,\theta,\ t)$~~, $M^i_{\mathrm{NASM}}$ ~~$(\lambda,\phi,\theta,\ t)$~~ and $M^i_{\mathrm{Tropics}}$ ~~$(\lambda,\phi,\theta,\ t)$ mark air mass fractions in the three-dimensional~~ mark source domains where the ~~artificial air fraction is~~ AOFs are set to 1 on each day during July−August in CLaMS simulations covering the period from 2010 to ~~2013. The~~ 2013 (the symbols $\lambda$, $\phi$ and t represent longitude, latitude and time, respectively~~. The tracer is~~). The AOFs are set to zero everywhere on 1 July of each year and ~~is~~ then set to 1 inside the corresponding source domains for this and every subsequent day through 31 August of ~~that~~ the same year. The artificial tracer is advected as an inert tracer ~~outside the source domains, as well as inside~~ inside and outside of the source domains after ~~the release. The tracer mixing ratio~~ its release, with advection driven by reanalysis horizontal winds and total diabatic heating rates. The AOF at any location in the stratosphere equals the mass fraction of air ~~which~~ (in %) that left the corresponding source layer in the ASM, NASM or tropical domain during the previous monsoon season~~(see also Orbe et al. 2013; Ploeger et al. 2017~~.

We run the simulation for the same period as Ploeger et al. (2017) to facilitate direct comparison between different definitions of the domain boundary (simplified box and PV-barrier). July and August represent the mature phase of the monsoon. We simulate transport from July-August instead of June-September to exclude substantial in-mixing of air from areas adjacent to the monsoon regions during the transitional months when the monsoon circulation is spinning up or spinning down (June and September) and avoid overestimating transport (Sensitivity to the length of the initialization period is discussed in more detail later in the paper). After releasing the tracer in each box, we ~~track the primary transport pathway and associated transport efficiencies~~ map the respective transport pathways from each source region to the global stratosphere, focusing especially on transport to the tropical pipe (TrP), the extratropical ~~lower~~ lowermost stratosphere in the Southern Hemisphere (LS-SH), and the extratropical ~~lower~~ lowermost stratosphere in the Northern Hemisphere (LS-NH). Note that transport from each source region is simulated independently. Therefore, there are no interactive influences among transport from the three source regions. This experimental setup is illustrated in Fig. 2.

Observations of the tropospheric tracer HCN obtained from the Atmospheric Chemistry Experiment Fourier Transform Spectrometer (ACE-FTS) satellite instrument (Bernath et al., 2005) are used to validate the artificial monsoon air mass tracer. These data have been presented and discussed by Randel et al. (2010) and Ploeger et al. (2017). Here, we use HCN from ACE-FTS level 2 data version 3.6 (Boone et al., 2005, 2013) to investigate the correspondence between pollutants in the stratosphere

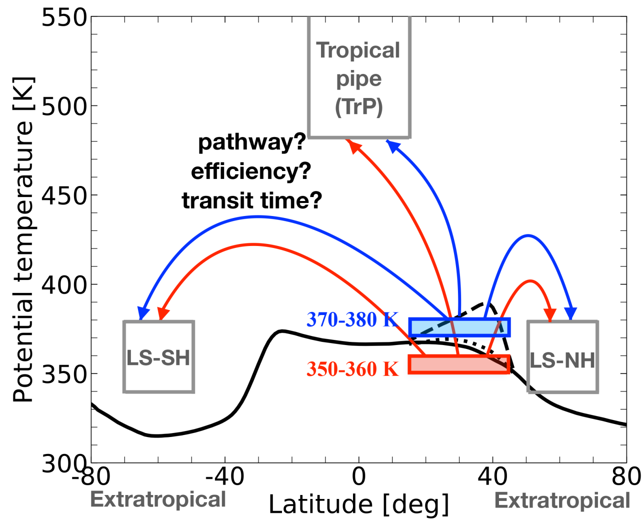


**Figure 2.** Definition of source regions ($\text{Box}_i$) at 350−360 K (red) and 370−380 K (blue). The following three destination regions (i.e. regions where transport statistics from the source regions are diagnosed) are considered: the tropical pipe (TrP: 15° S−15° N), the extratropical lower stratosphere in the Southern Hemisphere (LS-SH: 50° S−70° S), and the extratropical lower stratosphere in the Northern Hemisphere (LS-NH: 50° N−70° N). The black ~~solid,~~ dashed~~and~~, dotted, and solid lines respectively mark lapse rate tropopause locations within the ~~zonal-mean,~~ ASM ~~and~~ region, the NASM ~~tropopause (lapse rate)~~ region, and all other regions from ERA-Interim averaged over July−August 2010−2013.

and transport via both monsoons. In addition, MLS version 4 retrievals of CO (Livesey et al., 2018) are used to investigate the influence of the monsoon anticyclones on the tracer distribution as shown in Fig. 1b, and MLS version 4 retrievals of water vapor are used to diagnose vertical and horizontal transport of tracer from the monsoon regions and its influence on stratospheric composition.

## 3 Transport pathways into the stratosphere and influence on stratospheric composition

### 3.1 Zonal-mean perspective on transport

The evolution of the ASM tracer after its release is very similar to results shown by Ploeger et al. (2017, their Fig. 1). To avoid redundancy, we only show the AOF distributions around ten months after the tracers are initialized (i.e. during April-June), focusing on tracers that have been transported into the global stratosphere. Figure 3 shows the average ~~air mass fraction from~~ AOF from the ASM and NASM regions initialized in the 350−360 K (Fig. 3a and Fig. 3b) and 370−380 K (Fig. 3c and Fig. 3d) layers in July and August of 2010−2013 in the CLaMS-EI simulations during the following April−June~~, about ten months after the release of the tracers~~. These results are based on four sets of CLaMS simulations, with the AOF set to 1 in the 350−360 K or 370−380 K layer over the ASM or NASM region on each day during July−August. Air is transported

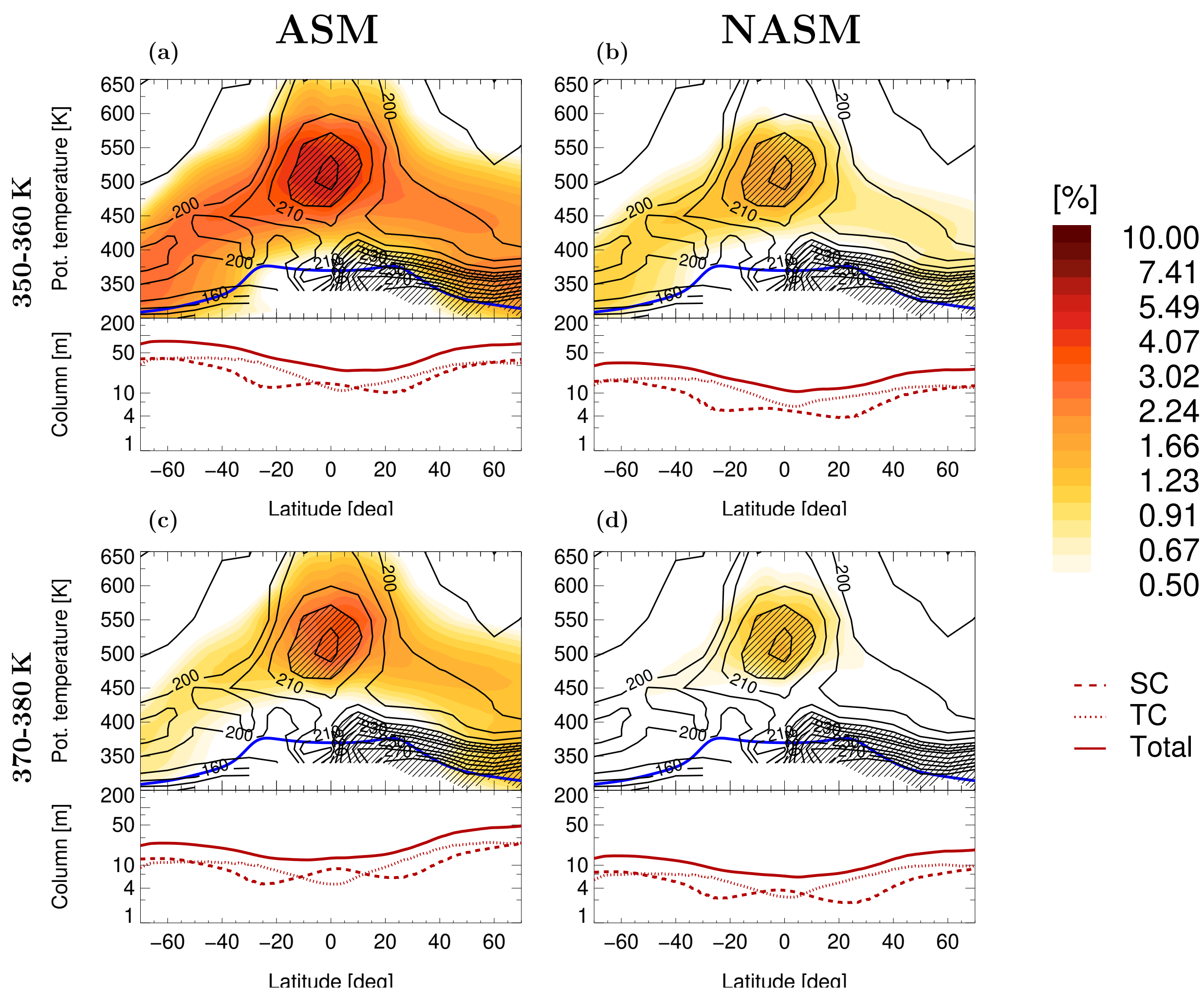


**Figure 3.** Climatological (2010−2013) zonal mean air mass origin fraction (AOF) from the ASM (a and c) and the NASM (b and d) initialized at 350−360 K (upper) and 370−380 K (lower) in July and August from CLaMS-EI (color shading) during the following April−June. HCN from ACE-FTS observations (black contours) is also shown~~for context~~. Regions with HCN volume mixing ratios greater than 215 pptv are hatched. Blue lines mark the lapse rate tropopause. The red lines show column integrals (thickness: in m) of the monsoon tracer above the tropopause (stratospheric column, SC: dashed), below the tropopause (tropospheric column, TC: dotted) and through the entire atmosphere (solid). ~~(~~Note the logarithmic color scale.~~)~~

to the global stratosphere from both the ASM and the NASM. However, much more monsoon air originates from the ASM region than from the NASM region, and ASM air is transported to a higher level in the TrP by the following April−June when compared to NASM air. More monsoon tracer is transported into the stratosphere from the 350−360 K layer than from the 370−380 K layer for both the ASM and NASM regions. Monsoon air initialized at 350−360 K is more prevalent in the SH stratosphere than in the NH, while monsoon air initialized at 370−380 K is more likely to remain in the NH. The distribution of ASM tracer initialized at 370−380 K (Fig. 3c) is similar to that reported by Ploeger et al. (2017, their Fig. 1d) based on a PV-barrier definition of the ASM, but the abundance of ASM air is greater in our results because our ASM domain is larger. The distribution of the monsoon tracer initialized at 340−350 K (not shown) is also skewed toward the SH, similar to the results for 350−360 K, while the distribution of the monsoon tracer from 360−370 K is more symmetric between the hemispheres. In summary, during the following April−June, the monsoon tracers are more likely to end up in the SH stratosphere if they are initialized at lower levels (340−350 K or 350−360 K), and more likely to end up in the NH stratosphere if they are initialized at higher levels (360−370 K or 370−380 K). To avoid redundancy, we only show the results for tracers initialized in the 350−360 K and 370−380 K layers in this paper.

Ploeger et al. (2017) showed that the simulated ASM tracer based on driving CLaMS with ERA-Interim correlates well with ACE-FTS observations of HCN. Here, we find that the HCN observations show strong correlations with both the ASM and NASM tracers in the TrP. This result suggests that both monsoon regions could serve as sources of enhanced HCN to the stratosphere, with the ASM region representing a relatively strong source and the NASM region representing a relatively weak source. Although the HCN mixing ratio over the NASM is lower than that over the ASM, it is much higher than that over the tropics (Randel et al., 2010, their Fig. 1). The peak HCN mixing ratios in the TrP closely overlap with the peak contributions of monsoon tracers initialized in the 350−360 K layer, and are located slightly below the peak contributions of monsoon tracers initialized at 370−380 K. However, such vertical offsets should be interpreted with caution given likely overestimates of tropical upwelling in ERA-Interim (Dee et al., 2011; Wright and Fueglistaler, 2013; Ploeger et al., 2019; Tao et al., 2019).

Column integrals are calculated to further investigate the transport of the monsoon tracers. These integrals are defined as the thickness (in units of m) of pure monsoon air assuming standard temperature and pressure for each altitude. Column integrals of monsoon air above the tropopause (SC), below the tropopause (TC), and through the entire atmosphere are shown along the bottom of each panel in Fig. 3. The column integrals of ASM and NASM tracers show similar patterns in both hemispheres. The TC, SC, and total monsoon tracer columns initialized at 350−360 K show slightly larger values in the SH. The larger columns in the SH originating from the 350−360 K layer over the boreal monsoon regions may arise from a combination of three effects: weaker confinement of air inside the monsoon regions at this layer (Garny and Randel, 2016; Vogel et al., 2019), hemispheric differences in isentropic mixing (Orbe et al., 2013; Konopka et al., 2017), and the seasonality of the Brewer-Dobson circulation (Seviour et al., 2011; Konopka et al., 2015). A portion of the monsoon tracers initialized at the 350−360 K level ~~enter~~ enters the tropics due to wave-driven isentropic transport~~and are~~, ascends through the tropical tropopause layer (TTL), and is then advected into the SH through the shallow branch of the Brewer-Dobson circulation (Rosenlof, 1995; Konopka et al., 2015). By contrast, monsoon tracers released in the 370−380 K layer are more tightly confined to the NH, with higher column-integrated values for both the troposphere and stratosphere in the NH.

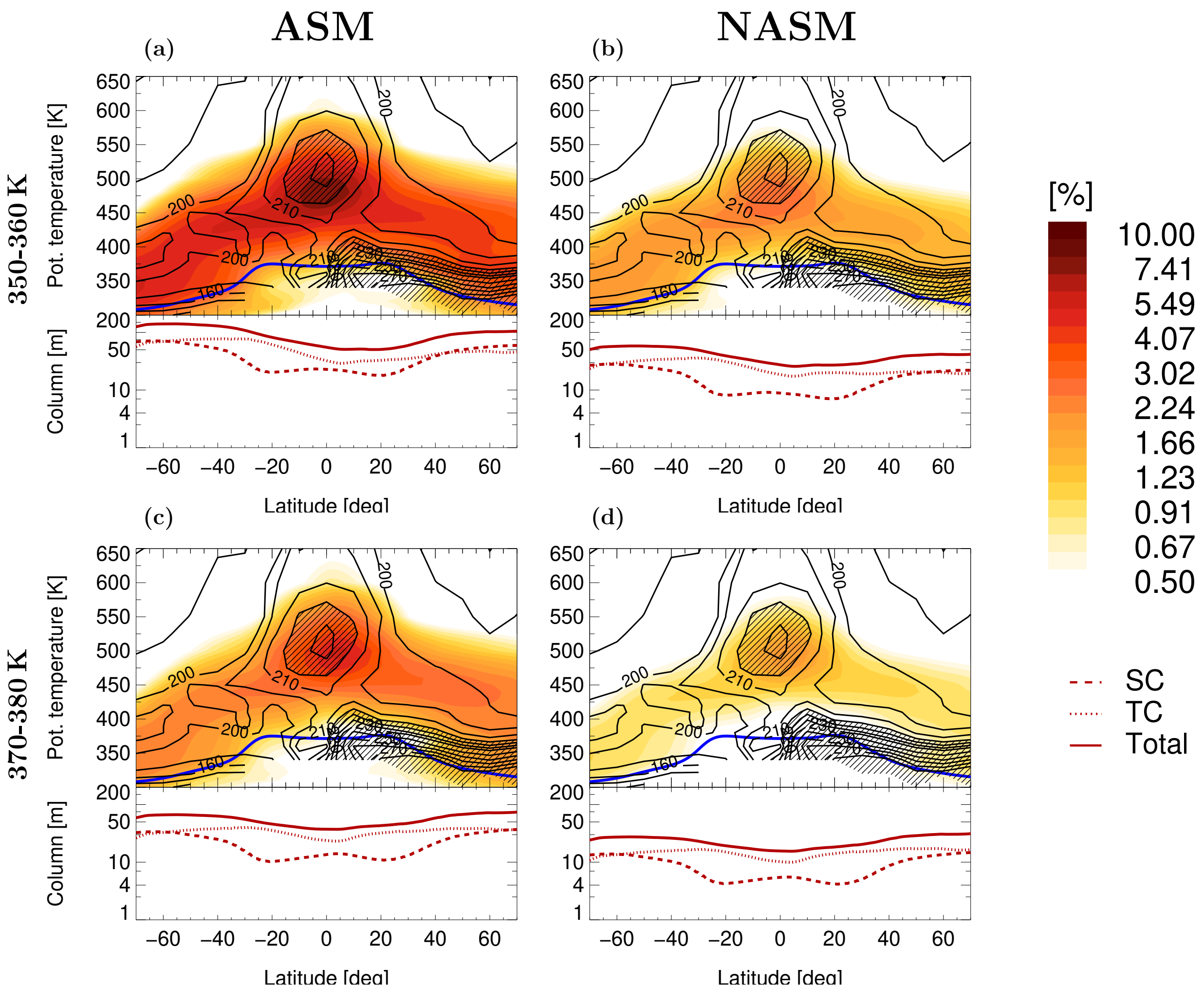


**Figure 4.** Same as Fig. 3 but for CLaMS-M2.

Figure 4 shows the ~~air fraction~~ AOF during the following April−June for the ASM and NASM tracers initialized at 350−360 K and 370−380 K in July−August based on CLaMS-M2 simulations. Similar to the results from CLaMS-EI, the fraction of ASM air is larger than that of NASM air in the TrP, and the ASM air reaches a higher vertical level. More monsoon tracer is transported into the stratosphere from lower levels than from higher levels, and the distributions of monsoon tracers also show hemispheric asymmetries similar to those in the CLaMS-EI case. However, despite these many similarities, the CLaMS-M2 simulations show much larger ~~proportions~~ fractions of ASM and NASM air in the global stratosphere in comparison to those from CLaMS-EI. Another prominent difference concerns the vertical transport of monsoon air. The tracer peak from CLaMS-M2 is slightly below the HCN peak from satellite observations for tracers initialized at both the lower and the upper layers. This can be attributed to slower upwelling, which stems from smaller diabatic heating rates in the lower stratosphere in MERRA-2 (Ploeger et al., 2019; Tao et al., 2019). Slower upwelling leads to larger contributions from quasi-horizontal transport and smaller contributions from vertical transport relative to the CLaMS-EI simulations. Transport of tracers into the stratosphere takes a longer time in the CLaMS-M2 simulations, but a larger fraction of monsoon air reaches and remains in the stratosphere. Column-integrated monsoon tracer values from CLaMS-M2 are also much larger than those from CLaMS-EI. This difference arises in part because monsoon tracers from CLaMS-M2 reach relatively lower ~~levels~~ altitudes in the stratosphere by the following April−June compared to those from CLaMS-EI and air density is larger at lower ~~levels~~altitudes. Differences between the SH and NH for monsoon tracers initialized in 370−380 K layer are smaller than those based on CLaMS-EI~~(not shown)~~.

### 3.2 Two distinct transport pathways

In Sec. 3.1, we ~~reported distinct~~ have discussed differences in transport into the stratosphere ~~between~~ from the ASM and ~~the NASM and between~~ NASM regions, focusing on two different vertical levels of the monsoon source regions in the upper troposphere (the 350−360 K and 370−380 K layers). The differences in simulated transport of monsoon tracers released at different vertical levels imply the existence of multiple transport pathways from the monsoon source regions to the TrP. Along the first pathway, termed ‘tropical pathway’ in the following, the tracer is first horizontally advected to the tropics, where it ascends through the ~~tropical tropopause layer (TTL )~~ TTL into the TrP. Along the second pathway, termed ‘monsoon pathway’ in the following, the tracer is first lifted across the tropopause within the monsoon anticyclone and then transported isentropically to the tropical lower stratosphere and TrP. In this section, we endeavour to disentangle these two pathways and clarify the extent of transport from the monsoon source regions to the global stratosphere by separating the contributions of vertical transport within the tropics from those of horizontal transport into the tropics. We also compare the artificial tracers from the model simulations with MLS water vapor observations and CLaMS-simulated water vapor to investigate the influence of the monsoons on stratospheric chemical composition.

The vertical transport of ASM and NASM air into the tropical stratosphere (15° S−15° N) in CLaMS-EI is illustrated using the familiar ‘tape-recorder’ form (Mote et al., 1996) in Fig. 5. The transport barrier between the tropics and subtropics is weaker during boreal summer (Chen, 1995; Haynes and Shuckburgh, 2000). Monsoon tracers released at lower levels are especially abundant in the tropical UTLS during summer, indicating that a large fraction of the monsoon air from 350−360 K ~~that reaches~~

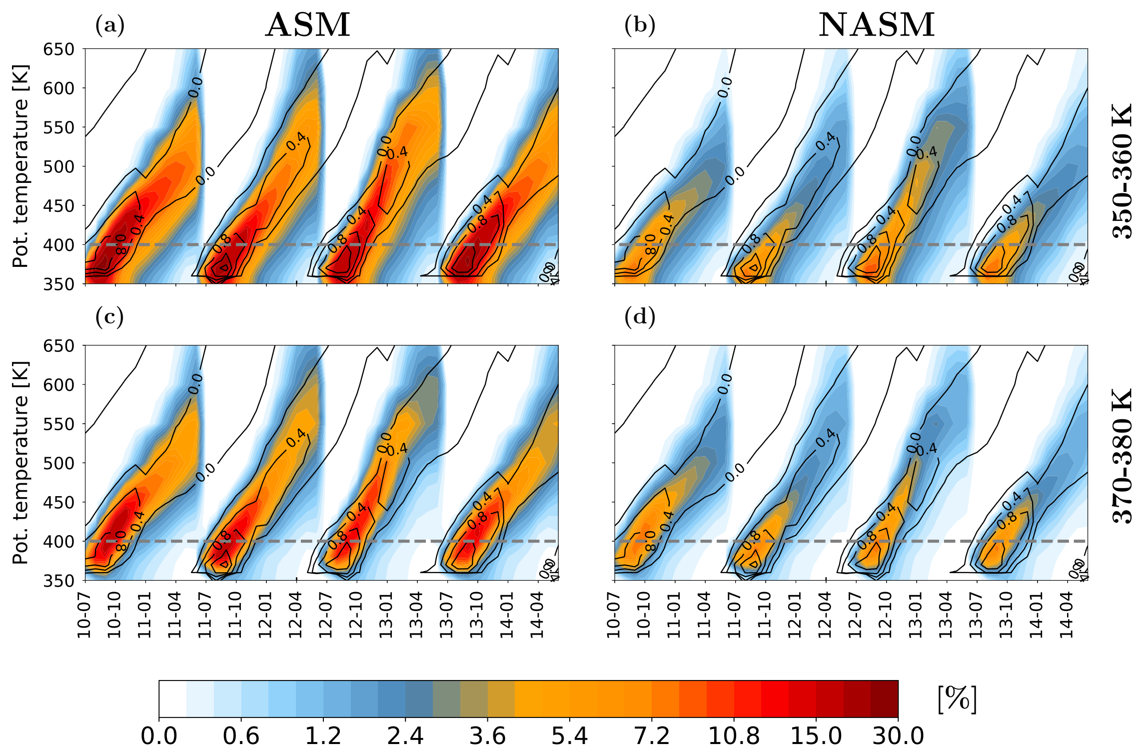


**Figure 5.** Potential temperature−time sections during July 2010 to June 2014 of ~~mean~~ zonal-mean monsoon air mass origin fraction (AOF: color shading) between 15° S and 15° N released in the 350−360 K (upper; a and b) and 370−380 K (lower; c and d) layers within the ASM (left; a and c) and NASM (right; b and d) based on CLaMS-EI simulations. Tape-recorder signals calculated from Aura MLS water vapor (in ppmv) with the annual average from each year removed are shown as black contours for context. Grey dashed lines mark the 400 K level. Note that the tracer is set to zero everywhere on 1 July of each year.

reaching the TrP may be advected quasi-horizontally into the tropics before ascending, in agreement with previous results based on trajectories initialized at 360 K (Garny and Randel, 2016). We also find that less of the monsoon tracer reaches the tropics when it is initialized at higher levels relative to when it is initialized at lower levels. This difference suggests that tracers initialized at higher levels within the monsoon regions primarily ascend locally before being mixed or advected into the tropics. ASM air rises slightly faster than NASM air and reaches slightly higher altitudes by the end of the simulation period. These features are consistent with the results discussed above.

MLS water vapor observations are included for additional context in Fig. 5. The annual mean of MLS water vapor is removed to highlight the annually-repeating water vapor tape recorder. The simulated ASM and NASM tracers correlate well with the 'wet' phase of the tape recorder (positive anomalies after removing the annual mean), which starts each year in boreal summer. The close correspondence between the monsoon air mass tracers and the 'wet' phase of the water vapor tape recorder in the tropics is consistent with the idea that the ASM and NASM contribute to moistening the tropical lower stratosphere during boreal

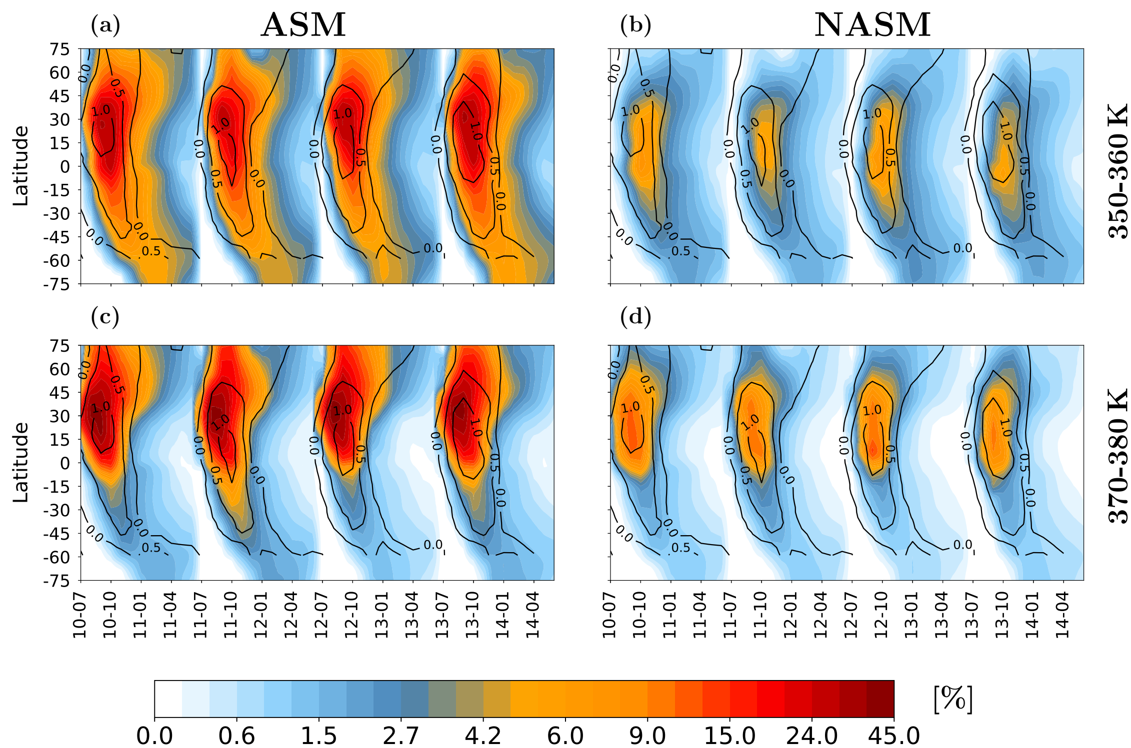


**Figure 6.** Zonal-mean tracer concentrations (color shading) for the ASM (left; a and c) and NASM (right; b and d) tracers initialized at 350−360 K (upper; a and b) and 370−380 K (lower; c and d) as functions of time and latitude on the 400 K isentropic surface based on CLaMS-EI (see also Fig. 5). MLS water vapor retrievals (in ppmv) with the annual average from each year removed are shown as black contours for context. Note that the tracer is set to zero everywhere on 1 July of each year.

summer ~~(Fu et al., 2006; Randel et al., 2012). Note however~~ (e.g. Dethof et al., 1999; Bannister et al., 2004; Fu et al., 2006; James et al., 2 . Note that large concentrations of monsoon tracers in the tropics do not always correlate with large water vapor mixing ratios in the tropical UTLS, as water vapor content at these altitudes depends not only on the origin of the air parcel but also on its temperature history (Fueglistaler and Haynes, 2005; Nützel et al., 2019).

CLaMS-M2 simulations (not shown) have much in common with the CLaMS-EI results with respect to the transport of monsoon tracers into the tropics. However, there are also some differences. As mentioned above, the vertical transport of the ASM tracers is slightly ~~lower~~weaker, with the tracers reaching slightly lower altitudes by the end of the simulation period. ~~Perhaps~~ Likely linked to this slower upwelling, more monsoon air arrives in the tropics between each summer monsoon season and the following spring compared to CLaMS-EI simulations. A relatively large ~~proportion~~ fraction of monsoon air is transported quasi-horizontally into the tropics before ascending to the TrP. The slower upwelling in MERRA-2 also manifests in a slight lag between the simulated monsoon tracer distribution and the MLS water vapor tape recorder signal.

~~Figure 6 shows~~ To investigate the influence of transport from the boreal monsoon regions on the lowermost stratosphere, we examine the horizontal spread of the ASM and NASM tracers on the 400 K isentropic surface based on the CLaMS-EI simulations (Figure 6). Tracers initialized on both levels show broadly similar features at 400 K, although the ASM contributes much more to the lower stratosphere than does the NASM. The ASM and NASM tracers initialized at 350−360 K are less confined in latitude, with much more transport to the SH than tracers initialized at 370−380 K. Tracers initialized at 370−380 K are more confined to the monsoon region and the NH, consistent with trajectory simulations initialized at 380 K (Garny and Randel, 2016). The ASM and NASM tracers coincide well with the MLS water vapor 'wet' signal in the lateral tape recorder, which is again consistent with the idea that the monsoons contribute substantially to water vapor concentrations in the stratosphere. The monsoon tracer distributions based on CLaMS-M2 are more widespread than those based on CLaMS-EI, with a greater tendency to remain in the extratropical stratosphere regardless of the initialization level. Both sets of simulations produce close matches between the ASM and NASM tracer peaks and the 'wet' signal in MLS water vapor, indicating that horizontal transport in CLaMS-M2 is in good agreement with that in CLaMS-EI.

The qualitative correspondence between the monsoon tracers and the 'wet' phases of the vertical and horizontal tape recorders suggests a strong connection between stratospheric water and transport from the monsoon regions. To further investigate the extent to which the monsoon tracers can explain variability in lower stratospheric water vapor and clarify the differences between the tropical pathway and the monsoon pathway into the TrP, we correlate the monsoon tracer amounts with CLaMS-simulated concentrations of stratospheric water vapor, which have been successfully validated and used in many previous studies ~~(e.g. Rolf et al., 2018; Tao et al., 2019, and the reference therein)~~(e.g. Vogel et al., 2016; Rolf et al., 2018; Tao et al., 2019, and . We analyse the data from November to May, i.e. about 4−10 months after the release of the monsoon tracers (as discussed below, this is the earliest that the tracers may reach the TrP). As shown in Fig. 7, a strong positive correlation exists between the monsoon tracers and water vapor in the tropics. Larger ASM and NASM air fractions correspond to larger water vapor mixing ratios in the tropical lower stratosphere (420−500 K). The distinct differences between the upper panels (tracers released in the 350−360 K layer) and the lower panels (tracers released in the 370−380 K layer) reflect the two transport pathways from the ASM and NASM to the tropical lower stratosphere. The right branch in Fig. 7a (Fig. 7b) mimics the joint distribution of ASM (NASM) tracers from 370−380 K and water vapor shown in Fig. 7c (Fig. 7d). This branch thus indicates the correlation along the monsoon transport pathway (cyan arrow), in which air ascends locally across the tropopause and then enters the tropics laterally. The left branch in Fig. 7a (Fig. 7b) is then linked to the correlation along the tropical pathway (magenta arrow), in which air from the upper troposphere above the ASM (NASM) region enters the tropics quasi-horizontally before ascending via tropical upwelling. ~~As discussed above, this~~

The tropical pathway is more common for tracers released at ~~lower altitudes (here~~ 350−360 K~~)~~. Most of the monsoon tracers released at 370−380 K are transported to the TrP along the monsoon pathway, although the tropical pathway is not completely absent for tracers released in this layer. The monsoon pathway coincides well with the upward spiraling range highlighted by Vogel et al. (2019). The water vapor mixing ratio along the tropical pathway is lower than that along the monsoon pathway because more dehydration is caused by the lower tropopause temperature over the tropics (figure omitted). The mass fraction of air younger than nine months is also shown in Fig. 7 (black contours) to further evaluate the vertical components of the

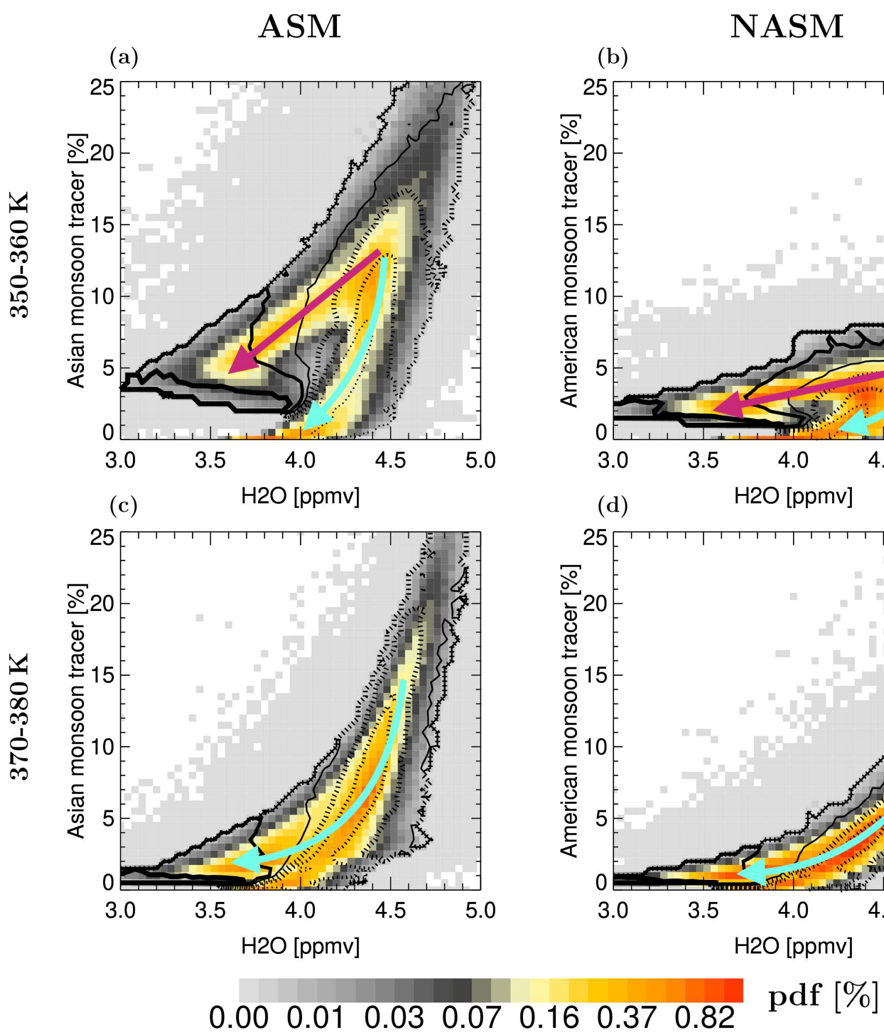


**Figure 7.** Correlations between CLaMS-simulated water vapor and the ASM (left; a and c) and NASM (right; b and d) tracers in the tropical stratosphere (15° S−15° N; 420−500 K) during from November —2010 to May 2011 with monsoon tracers released in the 350−360 K (upper; a and b) and 370−380 K (lower; c and d) layers based on CLaMS-EI. Contours mark young (less than nine months) air mass fractions of 24%, 33%, and 42% (from thin to thick dotted isolines) and 51%, 60%, and 69% (from thin to thick solid isolines). The cyan and magenta arrows respectively show the monsoon pathway and tropical pathway.

pathways by which monsoon air reaches the tropical lower stratosphere. Young air mass fractions are considerably larger for the tropical pathway, suggesting that overall ascent rates over the tropics (along the tropical pathway) are much faster than those over the monsoon regions (along the monsoon pathway) until the next early summer. Here, a single one-year simulation is used for each tracer because interannual variability obscures the structure in the correlation between water vapor and monsoon tracers. Results from other years are similar (not shown).

## 4 Transport budget

In this section, we investigate the total budget ~~and~~ (in terms of the AOF) and the efficiencies of transport from different layers over the monsoon source regions into the global stratosphere. Three destination regions as defined in Fig. 2 are of particular interest: the tropical pipe (TrP), the extratropical lower stratosphere in the NH (LS-NH) and the extratropical lower stratosphere in the SH (LS-SH). Because transport across the TTL is generally regarded as the 'main gateway into the stratosphere' (Fueglistaler et al., 2009), we compare the ASM- and NASM-related transport metrics with corresponding quantities calculated for a pure tropical source region (15° S−15° N).

### 4.1 Time evolution of the monsoon tracer

Figure 8a shows CLaMS-EI time series of the ASM tracer in the three destination regions (TrP, LS-NH and LS-SH) defined in Fig. 2. The ASM tracer initialized at 370−380 K ~~show~~ shows the largest air fraction in the LS-NH in the middle of September, with a peak value around 22%. The peak date is earlier than that shown by ~~Ploeger et al. (2017)~~ (Ploeger et al., 2017, their Fig. 2) (peak around 15%). This is because the geographical domain of the ASM tracer used here is larger than that based on the PV barrier ~~definition~~ defintion used by Ploeger et al. (2017). ~~Our definition of the LS-NH destination region also differs slightly from theirs. Our use of a geographical definition for the ASM as opposed to the dynamical definition used by Ploeger et al. (2017) means that some air parcels are initialized with ASM tracer when they are outside of the dynamical anticyclone . These parcels~~ As a consequence, air parcels that are not well confined inside the anticyclone may reach the LS-NH ~~much more quickly~~faster. The ASM tracers released in the 350−360 K layer show two peaks in the LS-NH. The first of these is at the beginning of September and is related to rapid isentropic poleward transport. The second occurs about one month later relative to the tracers initialized in the 370−380 K layer due to the need for additional (spiraling) ascent within the anticyclone (Ploeger et al., 2010; Garny and Randel, 2016; Vogel et al., 2019). During the first three months, fewer ASM tracers released at 350−360 K are diagnosed in the LS-NH relative to ASM tracers released at 370−380 K. However, after three months the ASM tracers released at 350−360 K contribute significantly more to the composition in the LS-NH and remain in the LS-NH for longer when compared to tracers released at 370−380 K~~after three months~~. Similar transitions in the relative concentrations of tracers released at 350−360 K and 370−380 K can be diagnosed in the TrP region, although the maxima are about six months later compared to ~~that~~ those in the LS-NH. The ASM tracers start to reach the TrP region around November, peaking in the TrP around March at a value ∼4% for tracers released in the 370−380 K layer. The timing of this peak is about

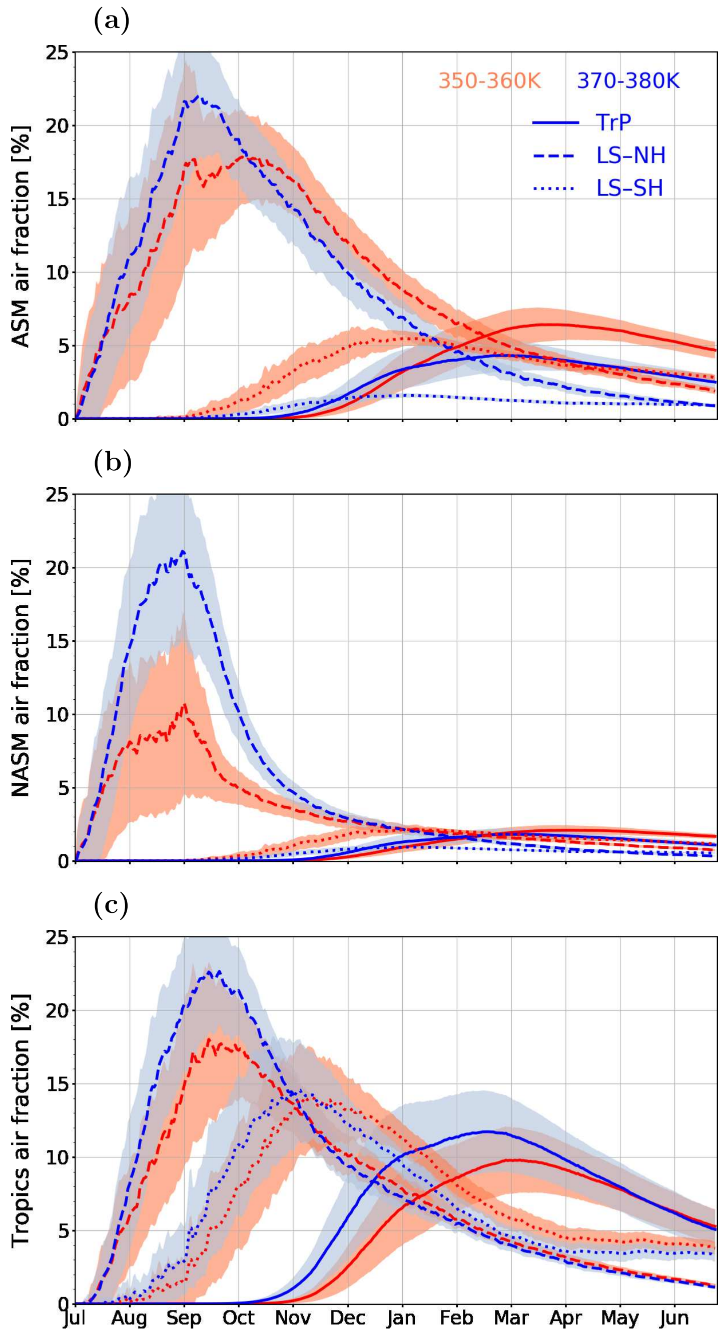


**Figure 8.** Climatological time series based on ~~the~~ CLaMS-EI simulations of air mass origin fractions (AOFs, in %) from the three source regions: (a) ASM, (b) NASM and (c) tropics ~~air mass fractions (in %) and~~ as diagnosed in three destination regions (see Fig. 2): tropical pipe (TrP, solid line), extratropical lower stratosphere in the NH (LS-NH, dashed line) and in the SH (LS-SH, dotted line). Shading shows the mean standard deviation in the zonal average (multiplied by ~~0.2~~ 0.5 for better visibility). Red and blue lines respectively represent the tracers released in the 350−360 K and 370−380 K layer.

half a month earlier than that of ASM tracers released from 350−360 K, although the latter has a larger peak value (∼7%). Tracers released at 350−360 K are much more abundant in the LS-SH than tracers released at 370−380 K throughout the year.

The corresponding time series of air fractions from the NASM source region to the three destination regions are illustrated in Fig. 8b. These time series show some important similarities to those based on the ASM tracers. The NASM tracers initialized in both the 350−360 K and 370−380 K layers reach their peak values in the LS-NH about two weeks earlier than the corresponding ASM tracer concentrations, likely owing to the weaker dynamical confinement of NASM air in the upper troposphere ~~.~~ ~~NASM tracers~~ (see also Fig. 1d). The amount of NASM tracer initialized at 370−380 K ~~reach~~ that reaches the LS-NH ~~in much larger amounts than NASM tracers~~ (21%) is similar to the amount of ASM tracer initialized at the same vertical layer that reaches the LS-NH. This similarity is also manifest in the comparable CO concentrations along 90° E and 90° W in the LS-NH (Fig. 1c and Fig. 1d). The amount of NASM tracer initialized at 350−360 K is much less, in part because the 370-380 K layer is ~~higher than the tropopause over the NASM~~ above the tropopause in the NASM region. However, NASM air fractions in the LS-SH and TrP are much smaller than the corresponding ASM air fractions in these regions, generally by more than a factor of 2. As for the ASM, NASM tracers initialized at 350−360 K are more abundant in the three destination regions by the end relative to NASM tracers initialized at 370−380 K.

Most tropospheric air that is transported into the global stratosphere passes through the TTL via tropical upwelling. Thus, to evaluate the relative contributions of the ASM and NASM sources to the stratosphere, we use the transport of air originating in the same vertical layers over the tropics (15° S − 15° N) as a benchmark. By comparing tracers tracking air of tropical origin in the three destination regions (Fig. 8c) with those tracking air with monsoon origin in the same destination regions, we conclude that ASM tracers are as abundant as tropical tracers in the LS-NH. Moreover, the abundance of the NASM tracer initialized in the 370−380 K layer is also comparable to the abundances of ASM or tropical tracers in the LS-NH region. Inside the TrP, the peak ASM contribution is smaller than the peak tropical contribution in early spring. However, the abundance of ASM air originating from 350−360 K in the TrP is comparable to that from the tropics at the end of the simulation period. Both values are about three times larger than the NASM contribution. ~~More~~ Much more air in the LS-SH originates from the tropical upper troposphere than from the two monsoon regions.

The time series of all source air fractions discussed above ~~and~~ calculated from CLaMS-M2 are very similar to those derived from CLaMS-EI (not shown). Even daily perturbations of such tracers driven by Rossby waves and diagnosed on individual isentropic surfaces show very strong similarities, as outlined later. ASM contributions based on CLaMS-M2 lag those based on CLaMS-EI by about one month, first reaching the TrP in December rather than November. This delay is related to the slower tropical upwelling in MERRA-2 relative to ERA-Interim as discussed above. For the same reason, CLaMS-M2 produces larger amounts of ASM tracers in the stratosphere at the end of the simulation period. The time series of NASM tracers based on CLaMS-M2 are likewise similar to those based on CLaMS-EI, again ~~up to and~~ including daily variability. For the tropical source, CLaMS-M2 shows similar peak values to CLaMS-EI in the LS-SH destination region, but lower peak values in the LS-NH and TrP. However, the amount of air of tropical origin ~~remaining in the stratosphere~~ reaching the TrP is larger in CLaMS-M2 than in CLaMS-EI starting from ~~the Aprilfollowing the July−August tracer release~~April.

| ERA-Interim | 340−350 K | 350−360 K | 360−370 K | 370−380 K |
|---|---|---|---|---|
| ASM | $2.276\times10^{10}$ | $1.877\times10^{10}$ | $1.179\times10^{10}$ | $6.118\times10^{9}$ |
| NASM | $1.916\times10^{10}$ | $1.042\times10^{10}$ | $5.649\times10^{9}$ | $3.930\times10^{9}$ |
| Tropics | $\cancel{8.524}1.188\times10^{\cancel{10}\,11}$ | $\cancel{5.484}5.950\times10^{10}$ | $\cancel{3.406}2.743\times10^{10}$ | $\cancel{2.207}1.621\times10^{10}$ |
| **MERRA-2** | **340−350 K** | **350−360 K** | **360−370 K** | **370−380 K** |
| ASM | $2.284\times10^{10}$ | $1.890\times10^{10}$ | $1.124\times10^{10}$ | $6.334\times10^{9}$ |
| NASM | $2.006\times10^{10}$ | $9.868\times10^{9}$ | $5.927\times10^{9}$ | $3.993\times10^{9}$ |
| Tropics | $\cancel{8.795}1.286\times10^{\cancel{10}\,11}$ | $\cancel{5.420}5.465\times10^{10}$ | $\cancel{3.398}2.908\times10^{10}$ | $\cancel{2.254}1.652\times10^{10}$ |

**Table 1.** Typical masses of air contained in each box for the test experiments over the ASM, NASM and tropical source regions in CLaMS-EI (top) and CLaMS-M2 (bottom). All masses are reported in kg.

### 4.2 Transport efficiency

Our comparison of ~~air fractions calculated for~~ AOFs conditioned on different transport pathways is partially hampered by the fact that the source regions have different ~~volumes (or masses)~~masses. To illustrate such differences in the domains, Table 1 shows the mass calculated for all considered source regions (ASM, NASM and tropics) based on both reanalyses. To better control for the potential influence of differences in the sizes of the source domains on our quantitative estimates of transport to the stratosphere, we define the efficiency of transport (TE) using the air mass of the source ~~domain~~ and destination domains, $m_{\mathrm{source}}$ and $m_{\mathrm{dest}}$, to normalize the mass transported from each source region to the defined stratospheric destination regions. Thus, TE is defined ~~to equal the mean source air mass fraction in the destination region times the total air mass of the destination region (e.g. TrP) divided by the air mass of the source domain (e.g. ASM)~~as AOF $\times\,(m_{\mathrm{dest}}/m_{\mathrm{source}})$.

Figure 9a compares the TE from the three source regions (ASM, NASM and Tropics) each divided into two layers (350−360 K and 370−380 K) to the LS-NH destination region. In contrast to the total budget, where tropical and monsoon contributions are very similar (Fig. 8), the ASM/NASM monsoons dominate the TE into the LS-NH, especially for sources in the 370−380 K altitude range. At the beginning, the TE is larger for the NASM than for the ASM; the larger NASM TE is in part related to the fact that the 370−380 K layer is above the tropopause over the NASM region and the NASM tracers are less confined. However, transport from the ASM becomes most efficient starting from October. Perhaps more surprising, the TE into the LS-SH is also dominated by the ASM and NASM ~~monsoon sources~~ regions for tracers released at 350−360 K after a certain date (see Fig. 9b). For the first 4−5 months, the TE is larger from the tropics than from the monsoon regions, especially for tracers released between 370 K and 380 K. However, ~~from January on,~~ transport from the 350−360 K layers in the ASM and NASM regions reaches the LS-SH more efficiently than transport from the same layer in the tropics ~~(with the TE slightly larger~~ starting from December or January (with TE from the ASM ~~than~~ larger than that from the NASM). The time evolution of the

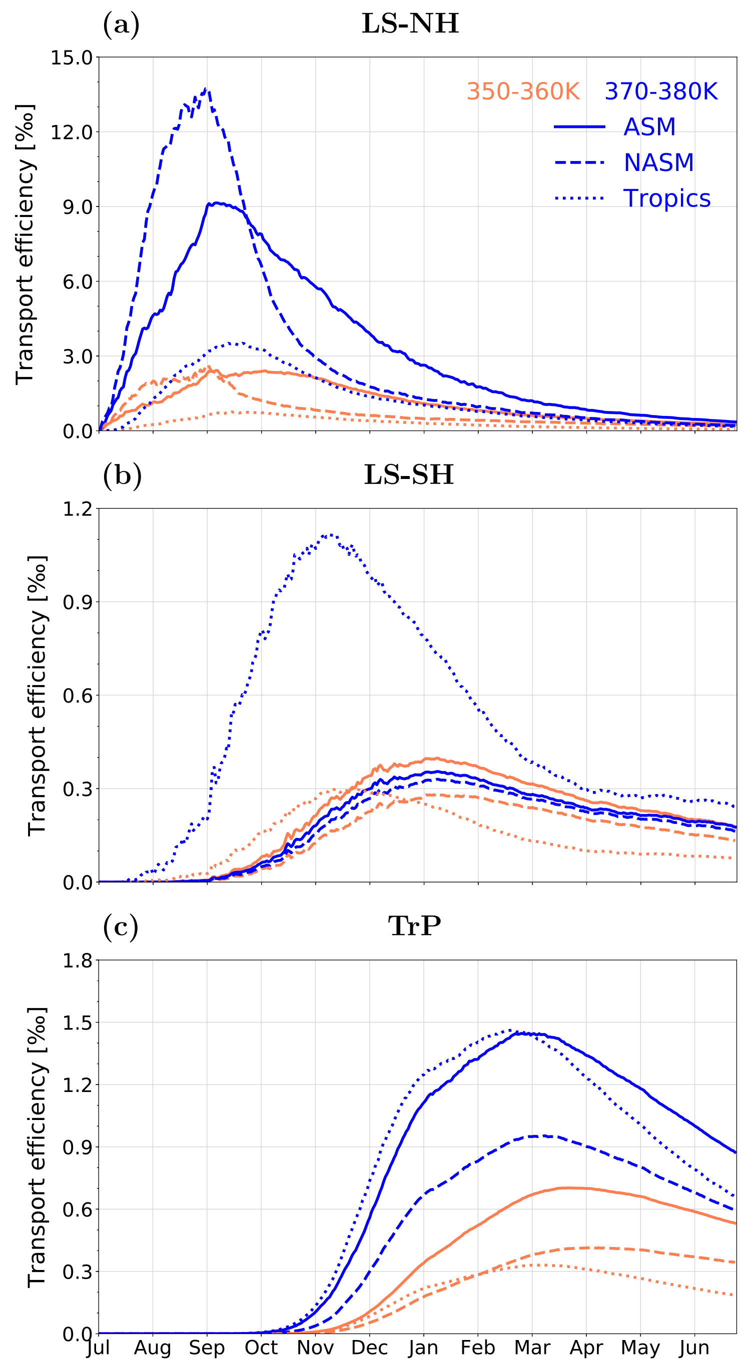


**Figure 9.** Climatological time series of transport efficiency (TE) as derived from the CLaMS-EI simulations and calculated for transport from the ASM (solid line), NASM (dashed line) and tropics (dotted line) source regions to the (a) LS-NH , (b) LS-SH and (c) TrP destination regions. TE (in ‰) is defined ~~by normalizing the average monsoon or tropical air mass over the destination region by~~ as AOF $\times$ $(m_{\mathrm{dest}}/m_{\mathrm{source}})$, where $m_{\mathrm{source}}$ and $m_{\mathrm{dest}}$ are the ~~mass~~ masses of the source ~~region~~and destination regions, respectively. Different colors of the lines represent tracers released at different levels.

source-resolved TE into the TrP is shown in Fig. 9c. Here, the highest TE values are along the pathways starting in the ASM source region after some certain date, followed by those starting in the tropical and NASM source regions. The NASM TE exceeds the tropical TE ~~after~~ by March for tracers from 350−360 K~~and after April for tracers from 370−380 K~~~~:~~. In contrast to the total source budget (Fig. 8), transport is consistently less efficient from lower levels than from higher levels.

Patterns of TE based on CLaMS-M2 are similar to those based on CLaMS-EI (~~figure omitted~~not shown), although there are a few important differences. First, TEs from the ASM and NASM source regions to the LS-SH destination region are much larger in CLaMS-M2 than in CLaMS-EI. Both values exceed ~~that~~ those from the tropical source region ~~after~~ by December (for tracers initialized at 350−360 K) or ~~January~~ February (for tracers initialized at 370−380 K). Second, the TE to the TrP in CLaMS-M2 shows slightly higher values for both the ASM and NASM sources and lower values for tropical upwelling relative to CLaMS-EI. TE from the NASM to the TrP slightly exceeds that from the tropics to the TrP starting in March (April) for tracers initialized at 350−360 K (370−380 K).

## 5 Discussion

~~We have investigated the pathways, transit times and efficiencies of transport from the ASM and NASM regions to the stratosphere with tracers initialized at different vertical levels using the ERA-Interim and MERRA-2 reanalyses. Both of the simulations show~~ The CLaMS-EI and CLaMS-M2 simulations both show that two major pathways~~connecting~~, here referred to as the monsoon and tropical, connect the upper troposphere in the ASM and NASM regions ~~to the TrP, as well as positive correlations between monsoon air mass fractions and MLS water vapor~~with the TrP. We have further shown that ~~contributions~~ the AOF from the ASM upper troposphere (350−360 K) to the TrP ~~are comparable to those of tropical sources~~ is comparable to the AOF from the tropical upper troposphere ten months after the ~~release of the tracers and that the~~ tracers are released. The most efficient transport to the TrP among the analyzed source regions is that from the ASM at 370−380 K. These robust characteristics of transport in the CLaMS-EI and CLaMS-M2 simulations are based on zonal-mean metrics.

To further investigate the sensitivity of the results to the choice of reanalysis, ~~zonally resolved results from the two sets of simulations are shown in Fig. 10. Figure 10 shows~~ zonally-resolved distributions of ASM tracers initialized in the 370−380 K layer ~~along~~ are shown for the 380 K isentropic surface on 24 August ~~2012. Distributions are shown for both~~ 2012 based on CLaMS-EI ~~(Fig. 10a)~~ and CLaMS-M2 (Fig. 10~~b~~). The ASM tracer is transported as far north as 75° N by eddies that detach from the ASM anticyclone. This type of feature is associated with Rossby wave breaking and can cause large fluctuations of monsoon air fraction in the LS-NH region (e.g. Popovic and Plumb, 2001; Ploeger et al., 2013; Vogel et al., 2014; Ungermann et al., 2016; . The consistency ~~between the~~ of CLaMS-EI and CLaMS-M2 ~~results for this case again~~ suggests good agreement between ~~CLaMS-EI and CLaMS-M2~~ these two simulations with respect to horizontal transport (see also Sec. 3.2). CLaMS-EI and CLaMS-M2 also show good agreement with respect to the horizontal distributions of monsoon tracers on other days (not shown). We select this example because it represents a clear episode of Rossby wave breaking and eastward eddy shedding.

Despite ~~the~~ many similarities in ~~simulated transport from the monsoon regions to the stratosphere in~~ the simulated transport between CLaMS-EI and CLaMS-M2, ~~it has been reported elsewhere that~~ there are also significant differences. As discussed

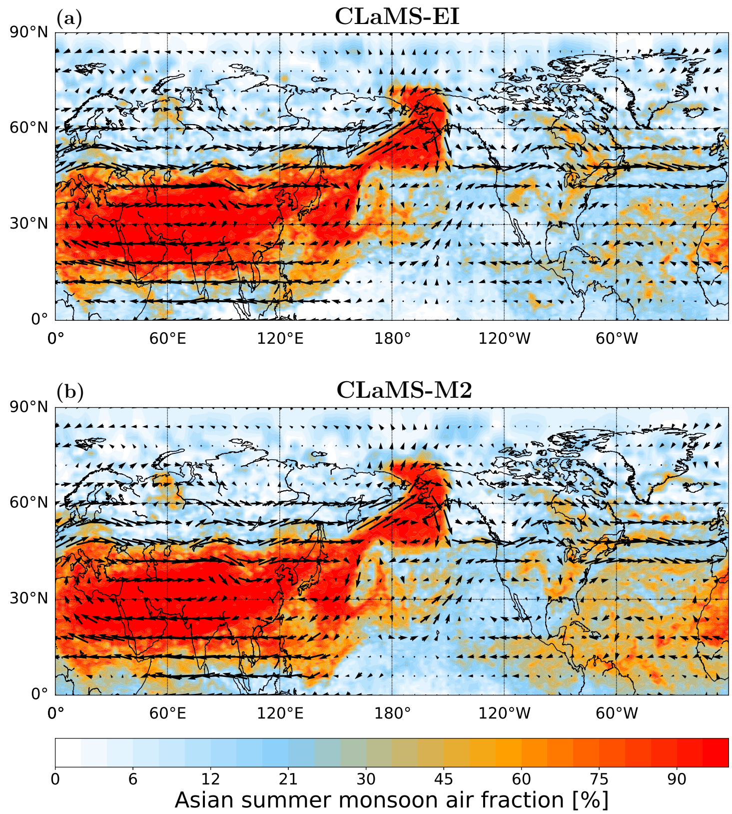


**Figure 10.** ~~The~~ A snapshot of the horizontal distribution of ~~(a) CLaMS-EI and (b) CLaMS-M2~~ the ASM tracer ~~simulation at~~ initialized in the 370–380 K layer on ~~24 August 2012 initialized at 370 –~~ the 380 K ~~from~~ isentropic surface on 24 August 2012 based on the ~~ASM region~~(a) CLaMS-EI and (b) CLaMS-M2 simulations. Arrows show horizontal wind ~~. Map is created by python~~on the same isentropic surface.

recently by Tao et al. (2019) and Ploeger et al. (2019), radiative heating rates in the TTL and lower stratosphere are substantially larger in ERA-Interim than in MERRA-2~~(e.g. Ploeger et al., 2019; Tao et al., 2019)~~. This difference directly affects the tropical upwelling as represented in CLaMS. We have shown that the monsoon tracers reach different maximum altitudes in the TrP during April–June in these two simulations. The stronger tropical upwelling in CLaMS-EI lifts monsoon air to higher altitudes more quickly than the weaker tropical upwelling in CLaMS-M2. Accordingly, the transit time to a given altitude in the TrP is slightly shorter in CLaMS-EI than in CLaMS-M2. Moreover, the smaller magnitudes of heating rates (both positive and negative) in CLaMS-M2 ~~tend to~~ lead to monsoon air ~~'piling up'~~ accumulating in the lowermost stratosphere and TrP (Fig. 4). Monsoon tracers thus retain high values in the stratosphere for longer in the CLaMS-M2 simulations. Slower cross-isentropic transport ~~increases the probability of~~ makes quasi-horizontal (isentropic) transport into the tropics ~~, where widespread upwelling helps to transport more air upwards~~more effective.

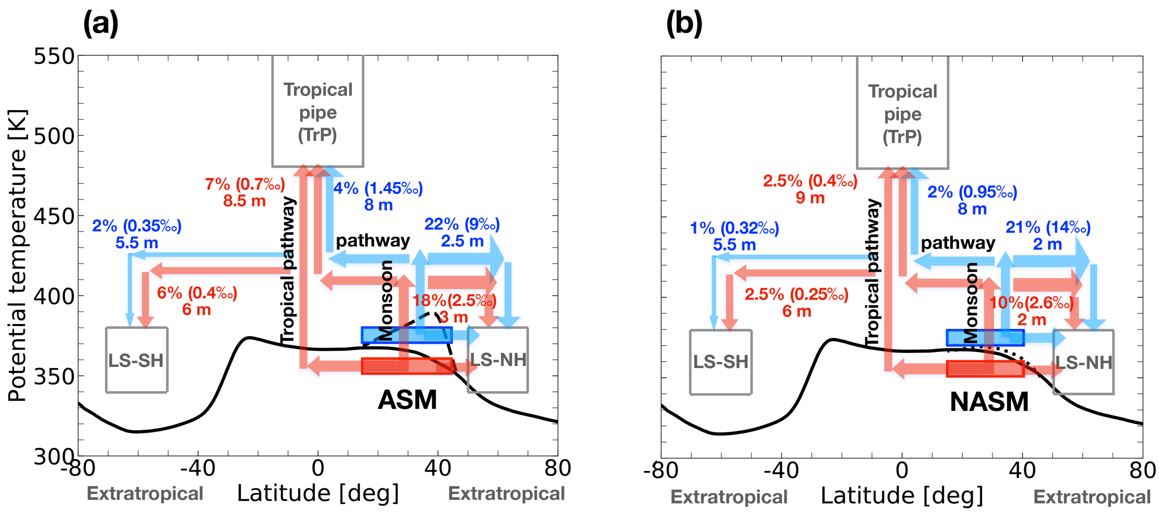


**Figure 11.** Schematic of tracer transport from the (a) ASM and (b) NASM region into the TrP, LS-NH and LS-SH. The red and blue boxes respectively represent the tracers initialized in the 350−360 K and 370−380 K layers. The arrows illustrate the dominant transport pathways. The numbers quantify the maximum ~~contribution %~~AOF (in %), the maximum transport efficiency (TE, in ‰) and the mean transit time (in month) from the monsoon regions to ~~the~~ three destination regions based on the CLaMS-EI simulations. The black ~~solid,~~ dashed~~and~~, dotted, and solid lines respectively mark lapse rate tropopause locations within the ~~zonal-mean,~~ ASM ~~and~~ region, the NASM ~~tropopause (lapse rate)~~ region, and all other regions from ERA-Interim averaged over July−August 2010−2013.

Another open question is the sensitivity of our results to the geometric definition of the source regions or to the length of the period during which monsoon tracers are initialized. To address this, we have conducted simulations with modified definitions of the ASM domain (by shifting the southern boundary to the north from 15° N to 20° N) and NASM domain (by shifting the western boundary to the east from 160° W to 120° W). The resulting tracer distribution patterns are very similar. Owing to the smaller sizes of the source domains, AOFs in the destination regions are smaller in these test cases than in the reference case, especially for transport from the NASM to the LS-NH. However, differences in TE are much less pronounced. This latter result is consistent with the definition of TE, which accounts for the sizes of the source and destination regions. The insensitivity of the results to the source domain boundary in our study is in agreement with the findings shown by Garny and Randel (2016), where they found that the differences are small regarding a change in the source region definition from PV-contour to box. If monsoon tracers are initialized from 15 June to 15 September instead of only from 1 July to 31 August, the abundances of monsoon air in the stratosphere are larger compared to the reference case. However, the transport patterns are very similar, including the hemispheric asymmetry in the distribution of monsoon tracers and the largest TE being associated with transport from the 370−380 K layer above the ASM. Hence, the conclusions of this study are qualitatively robust to reasonable definitions of the monsoon tracers.

Figure 11 provides a schematic illustration of the main transport pathways from the ASM (Fig. 11a) and NASM (Fig. 11b) source regions to the three stratospheric destination regions. The ~~overall contributions, efficiencies~~ average AOFs, TEs and transit times ~~along~~ associated with these pathways are also listed based on the CLaMS-EI results. The ~~greatest relative part, i.e.~~ largest contribution, representing about 22% (18%) of the air in the LS-NH, consists of ASM tracers initialized at 370−380 K (350−360 K), with an overall TE of 9‰ (2.5‰) and a transit time of ∼3 months. The contribution of the NASM tracers initialized at 370−380 K to the LS-NH is comparable to that of the corresponding ASM tracers, ~~although~~ while the contribution of the NASM tracers initialized at 350−360 K is much smaller than that of the ASM tracers initialized in the same layer. Although not shown here, these three quantitative transport metrics are quite similar ~~in~~ to CLaMS-M2 results with respect to transport from the ASM and NASM regions to the LS-NH. This similarity ~~supports our contention~~ confirms our finding that these two reanalyses provide very consistent representations of horizontal transport. A maximum of 7% of the air arrives in the TrP via the two main transport pathways (monsoon and tropical) from the 350−360 K layer in the ASM region. The transit time is about 8.5 months, with a peak efficiency of 0.7‰. The ASM tracers initialized at 370−380 K take about 8 months to arrive ~~at~~ in the TrP. Although only about 4% of the air in the TrP comes from ~~this source layer~~ the 370−380 K layer above the ASM, the peak transport efficiency (1.45‰) is approximately twice as high as that from the 350−360 K layer. Transport from ~~the source regions in the NASM shows much weaker contributions~~ source regions above the NASM contributes much less to air in the TrP, ~~along~~ with slightly longer transit times compared to transport from the ASM. ~~As for the NASM, the maximum contribution~~ The maximum contribution of the NASM is larger from the 350−360 K layer (2.5%) ~~but at a lower peak efficiency (0.4) relative to transport~~ than from the 370−380 K layer (2%~~and~~), but with a lower peak efficiency from lower layer (0.4‰relative to 0.95‰)~~. Our results about the contributions of monsoon air to the TrP and LS-NH are respectively smaller and larger than the results from Nützel et al. (2019) because the definitions of destination regions (TrP and LS-NH)used here are quite different from theirs.~~ .

Transit times from the monsoon regions to the TrP are about one month longer in the CLaMS-M2 simulations than in the ClaMS-EI simulations (not shown). The overall contributions and efficiencies of transport from the ASM and NASM to the TrP are also slightly larger in CLaMS-M2 than those in CLaMS-EI. The contributions from the ASM and NASM regions to the LS-SH are significantly different between tracers initialized at 350−360 K and tracers initialized at 370−380 K. ~~In both cases, the contributions from 350−360 K are almost three times larger than those from 370−380 K in CLaMS-EI. The scale of this difference is smaller in CLaMS-M2 than in CLaMS-EI.~~ Moreover, the absolute contributions based on CLaMS-M2 are much larger, with higher transport efficiencies and slightly longer transit times relative to CLaMS-EI. Since the tracers in the simulations are reset every July, we cannot infer how differences between CLaMS-EI and CLaMS-M2 evolve after June. ~~However, based on the tendencies toward the end of the simulation period, the concentrations of monsoon tracers in the stratosphere in CLaMS-M2 may decrease further in time, coming into better agreement with CLaMS-EI, until the point when the signature of the new monsoon season arrives.~~

Nützel et al. (2019) recently quantified water vapor transport from the ASM and NASM regions to the stratosphere by using CLaMS-EI simulations in a similar configuration. In our approach as well as that of Nützel et al. (2019), tracers are initialized in the upper troposphere above 350 K to reduce the impact of small-scale transport processes in the troposphere (e.g. convection)

Source regions

| Publication | ASM | NASM | Release time | Vert. range |
|---|---|---|---|---|
| Our study | 15–45° N, 30–120° E | 15–40° N, 160–60° W | Jul–Aug, 2010–13 | 350–360 K, 370–380K |
| Nützel et al. | 15–40° N, 20–130° E | 15–40° N, 170–60° W | Jul–Aug, 2010–13 | 360–380 K |
| Vogel et al. | India+China | – | May–Oct, 2007–08 | ABL (0–3 km) |

Destination regions

| Publication | LS-NH | TrP |
|---|---|---|
| Our study | 50–70° N, 340–380 K | 15° S–15° N, 480–550 K |
| Nützel et al. | 50–70° N, 400 K | 10° S–10° N, 450 K |
| Vogel et al. | 360 K, PV>5.5; 380 K, PV>7.2 | 30° S–30° N, 550 K |

Comparison of transport

| Publication | ASM→LS-NH | NASM→LS-NH | ASM→TrP | NASM→TrP |
|---|---|---|---|---|
| Our study | 18%, 22% | 10%, 21% | 7%, 4% | 2.5%, 2% |
| Nützel et al. | 22% | 4.4% | 12% | 5.2% |
| Vogel et al. | 18%, 16% | – | 6% | – |

**Table 2.** Comparison of the setups (source, destination, time periods) and the respective AOFs in Vogel et al. (2019), Nützel et al. (2019) and our study.

with uncertain representations in global reanalysis data. Our findings are also comparable to those of Vogel et al. (2019), who also used CLaMS-EI but with full transport from the boundary layer to the stratosphere included. In Table 2, we summarize the methodologies (source, destination, time periods) and respective AOFs published by Vogel et al. (2019) and Nützel et al. (2019) in comparison with our results. The AOF from the NASM region to the LS-NH as reported by Nützel et al. (2019) is much smaller (4.4%) than 21% obtained in our study. The difference is due to different definitions of the LS-NH destination region (400 K level in Nützel et al. 2019; 340–380 K layer in our study), implying that transport from the NASM mainly affects the lowermost stratosphere, with relatively weak influences on the extratropical stratosphere above 400 K. Differences in AOF values quantifying transport to the TrP can also be explained by slightly different definitions of the TrP among these studies (see Table 2). However, while Nützel et al. (2019) restricted their analysis only to the monsoon pathway (by considering only transport from the 370–380 K layer), our study illustrates the importance of the tropical pathway in transporting air from the 350–360K layer in the monsoon regions to the TrP. On the other hand, Vogel et al. (2019) discussed the transport from the atmospheric boundary layer (ABL) over India/China to the TrP and did not distinguish between the tropical and monsoon pathways.

To more clearly separate the contributions of these two pathways to transport from the 350–360 K layer over the ASM to the TrP, we conduct an additional simulation in which we artificially suppress transport along the monsoon pathway by re-setting this tracer to zero in the 370–380 K layer over the ASM region through the full duration of the simulation. We

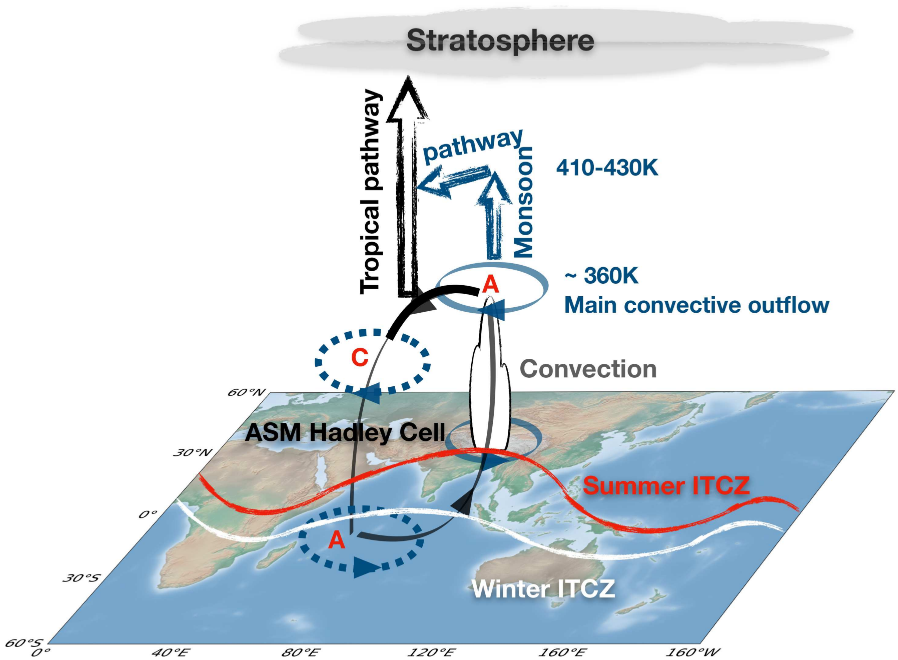


**Figure 12.** Schematic illustration of transport from ASM convective outflow along the main transport pathways to the stratosphere during boreal summer. The typical positions of the ITCZ and the monsoon Hadley cell are also shown.

find that more than 50% of the ASM tracers reaching the TrP (7% AOF) are transported via the tropical pathway (4% AOF). Moreover, the tropical pathway accounts for most of the transport from the ASM region to the LS-SH. The maximum AOF from the 350−360 K layer over the ASM to the LS-SH is 6%, of which more than 80% results from transport through the tropical pathway. Both tropical and monsoon pathways are schematically illustrated in Fig. 12. The strong heat source over Himalayas and Tibetan Plateau amplifies the northward shift of the ITCZ and forms the local monsoon Hadley circulation (Molnar et al., 1993; Pillai and Mohankumar, 2008). The tracers from convective outflow within the ASM region (∼360 K) can be transported to the tropics and even to the southern hemisphere via the upper-level cross-equatorial branch of the monsoon Hadley circulation, which is part of the tropical pathway in our study.

## 6 Conclusions

~~Both the CLaMS-EI and CLaMS-M2 simulations~~ We have investigated the pathways, transit times and efficiencies of transport from the ASM and NASM regions to the stratosphere with tracers initialized at different vertical levels and advection driven by the ERA-Interim and MERRA-2 reanalyses. Both types of simulation show that transport from the upper troposphere (350−360 K) over ASM and NASM regions makes a larger contribution to the TrP relative to transport from just below the tropopause (370−380 K). ~~This~~ Although part of the difference is related to the mass of air within each layer, which is larger for the 350−360 K layer than for the 370−380 K layer~~above the monsoon regions. Differences in the contributions of the two layers also arise due to vertical differences in the dynamical situation. Monsoon~~, there are also dynamical reasons related to the different strength of the anticyclone between these two levels. Thus, monsoon air mass fractions in the LS-SH and TrP during the following April−June are larger for tracers released at lower levels (350−360 K), reflecting weaker confinement by the anticyclone in the upper troposphere relative to just below the tropopause. By contrast, monsoon air fractions in the LS-NH region during the following April−June are larger for tracers released at higher levels (370−380 K), reflecting the importance of wave-driven transport of tracers that reach the extratropical lower stratosphere quasi-isentropically at higher levels.

Peak values of monsoon tracers in the tropical stratosphere are in good agreement with the 'wet' phase of the water vapor tape recorder based on Aura MLS, which is consistent with the monsoon regions playing an influential role in the seasonal cycle of water vapor in the tropical lower stratosphere. Differences between simulations with tracers initialized at 350−360 K and simulations with tracers initialized at 370−380 K suggest the existence of two main transport pathways between the monsoon regions and the TrP. The first pathway (tropical pathway) involves the quasi-horizontal transport of monsoon air into the tropics, where that air then ascends into the stratosphere via tropical upwelling. The second pathway (monsoon pathway) involves the ascent of monsoon air within the monsoon anticyclone into the lower stratosphere, where it is then transported quasi-horizontally to the tropical lower stratosphere. Both pathways ultimately reach the TrP. However, the greater abundance of relatively young air along the tropical (first) pathway suggests that vertical transport is faster along this route than along the monsoon (second) pathway after summer.

CLaMS-EI and CLaMS-M2 results consistently indicate that the ~~ultimate~~ average final contribution of air mass ~~transport~~ from the ASM ~~upper troposphere (~~350−360 K ~~)~~ layer to the TrP (~~∼5%~~i.e. at the end of simulation period for each year, when all the tracer are reset to zero) is comparable to that of direct ascent from the inner tropics (~~15° S–15° N)ten months after the release of the source tracers. These two contributions are~~ ∼5%). This contribution is approximately three times larger than the ~~air mass~~ respective contribution from the NASM (∼1.5%)~~to the TrP at the end of the simulation period. To help~~. To eliminate the influence of the origin/source region size on our quantitative transport estimates, we ~~calculate normalized transport efficiencies by dividing the total air mass transport by the average mass of air within the source domain~~also calculated the TE. The ASM region at 370−380 K shows the highest TE to the TrP (0.9‰)~~. Meanwhile, the~~ at the end of our simulation period. The respective TE from the NASM ~~to the TrP~~ is similar to ~~the TE from the tropics to the TrP (0.3–0.6). These values are approximately half that of the TE from the ASM to the TrP~~that from the tropics.

Our results further confirm the important role of the ASM anticyclone in troposphere-to-stratosphere transport. The maximum and final contributions as well the TE (Table 3) may help to explain, at least qualitatively, the stratospheric abundances of anthropogenic pollutants in relation to their lifetimes. Although the contribution from the NASM region to the TrP is less than the contributions from the ASM or from the tropics, it is still influential at about one third of the contribution from ASM. Moreover, the TE from the NASM to the TrP is as high as that of direct upwelling within the tropics during the boreal summer season.

*Data availability.* The MLS and ACE-FTS data are available at http://mirador.gsfc.nasa.gov and http://www.ace.uwaterloo.ca/data.php, respectively. The CLaMS model outputs may be obtained from the first author upon request.

*Author contributions.* XY carried out the ERA-Interim and MERRA-2 driven model simulations and the data analysis. PK, FP and AP contributed codes for the analysis. JW contributed codes to prepare the MERRA-2 reanalysis data. PK, FP and AP contributed to the design of the analysis. PK, FP, AP, JW, RM, MR provided helpful discussions and comments. XY wrote the paper with contributions from all co-authors.

*Competing interests.* The authors declare that they have no conflict of interest.

*Acknowledgements.* This research was partially supported by the National Key Research and development program of China (2018YFC1505703), the National Science Foundation of China (91837311, 41905040), and a joint DFG-NSFC research project with DFG project number 392169209 and NSFC project number 20171352419. We thank the European Centre for Medium-Range Weather Forecasts (ECMWF) and National Aeronautics and Space Admistration (NASA) for providing ERA-Interim and MERRA-2 meteorological reanalysis data for this study. We thank ~~MLS~~ the MLS team for providing CO and $H_2O$ data, and the ACE-FTS team for providing HCN data. ~~The MLS and ACE-FTS data are available at http://mirador.gsfc.nasa.gov and http://www.ace.uwaterloo. ca/data. php, respectively~~We thank Laura L. Pan for helpful discussions regarding the monsoon Hadley circulation. The authors would also like to thank the three anonymous reviewers for their very insightful comments.

## References


Abalos, M., Legras, B., Ploeger, F., and Randel, W. J.: Evaluating the advective Brewer-Dobson circulation in three reanalyses for the period 1979-2012, J. Geophys. Res., 120, doi:10.1002/2015JD023 182, 2015.

Anderson, J., Wilmouth, D., Smith, J., and Sayres, D.: UV Dosage Levels in Summer: Increased Risk of Ozone Loss from Convectively Injected Water Vapor, Science, 337, 835–839, https://doi.org/10.1126/science.1222978, 2012.

Bannister, R. N., O'Neill, A., Gregory, A. R., and Nissen, K. M.: The role of the south-east Asian monsoon and other seasonal features in creating the 'tape-recorder' signal in the Unified Model, Q. J. R. Meteorol. Soc., 130, 1531–1554, 2004.

Barth, M. C., Lee, J., Hodzic, A., Pfister, G., Skamarock, W. C., Worden, J., Wong, J., and Noone, D.: Thunderstorms and upper troposphere chemistry during the early stages of the 2006 North American Monsoon, Atmospheric Chemistry and Physics, 12, 11 003–11 026, https://doi.org/10.5194/acp-12-11003-2012, 2012.

Bergman, J. W., Jensen, E. J., Pfister, L., and Yang, Q.: Seasonal differences of vertical-transport efficiency in the tropical tropopause layer: On the interplay between tropical deep convection, large-scale vertical ascent, and horizontal circulations, J. Geophys. Res., 117, https://doi.org/10.1029/2011JD016992, 2012.

Bergman, J. W., Fierli, F., Jensen, E. J., Honomichl, S., and Pan, L. L.: Boundary layer sources for the Asian anticyclone: Regional contributions to a vertical conduit, J. Geophys. Res., 118, 2560–2575, https://doi.org/10.1002/jgrd.50142, 2013.

Bernath, P. F., McElroy, C. T., Abrams, M. C., Boone, C. D., Butler, M., Camy-Peyret, C., Carleer, M., Clerbaux, C., Coheur, P.-F., Colin, R., DeCola, P., DeMazière, M., Drummond, J. R., Dufour, D., Evans, W. F. J., Fast, H., Fussen, D., Gilbert, K., Jennings, D. E., Llewellyn, E. J., Lowe, R. P., Mahieu, E., McConnell, J. C., McHugh, M., McLeod, S. D., Michaud, R., Midwinter, C., Nassar, R., Nichitiu, F., Nowlan, C., Rinsland, C. P., Rochon, Y. J., Rowlands, N., Semeniuk, K., Simon, P., Skelton, R., Sloan, J. J., Soucy, M.-A., Strong, K., Tremblay, P., Turnbull, D., Walker, K. A., Walkty, I., Wardle, D. A., Wehrle, V., Zander, R., and Zou, J.: Atmospheric Chemistry Experiment (ACE) Mission overview, Geophys. Res. Lett., 32, L15S01, https://doi.org/10.1029/2005GL022386, 2005.

Boone, C. D., Nassar, R., Walker, K. A., Rochon, Y., McLeod, S. D., Rinsland, C. P., and Bernath, P. F.: Retrievals for the atmospheric chemistry experiment Fourier-transform spectrometer, Applied optics, 44, 7218–7231, 2005.

Boone, C. D., Walker, K. A., and Bernath, P. F.: Version 3 Retrievals for the Atmospheric Chemistry Experiment Fourier Transform Spectrometer (ACE-FTS), (Peter F. Bernath, editor, A. Deepak Publishing, Hampton, Virginia, U.S.A., 2013), 2013.

Brunamonti, S., Jorge, T., Oelsner, P., Hanumanthu, S., Singh, B. B., Kumar, K. R., Sonbawne, S., Meier, S., Singh, D., Wienhold, F. G., Luo, B. P., Boettcher, M., Poltera, Y., Jauhiainen, H., Kayastha, R., Karmacharya, J., Dirksen, R., Naja, M., Rex, M., Fadnavis, S., and Peter, T.: Balloon-borne measurements of temperature, water vapor, ozone and aerosol backscatter on the southern slopes of the Himalayas during StratoClim 2016–2017, Atmospheric Chemistry and Physics, 18, 15 937–15 957, https://doi.org/10.5194/acp-18-15937-2018, 2018.

Chen, P.: Isentropic cross-tropopause mass exchange in the extratropics, Journal of Geophysical Research: Atmospheres, 100, 16 661–16 673, https://doi.org/10.1029/95JD01264, 1995.

Chirkov, M., Stiller, G. P., Laeng, A., Kellmann, S., von Clarmann, T., Boone, C. D., Elkins, J. W., Engel, A., Glatthor, N., Grabowski, U., Harth, C. M., Kiefer, M., Kolonjari, F., Krummel, P. B., Linden, A., Lunder, C. R., Miller, B. R., Montzka, S. A., Mühle, J., O'Doherty, S., Orphal, J., Prinn, R. G., Toon, G., Vollmer, M. K., Walker, K. A., Weiss, R. F., Wiegele, A., and Young, D.: Global HCFC-22 measurements with MIPAS: retrieval, validation, global distribution and its evolution over 2005–2012, Atmospheric Chemistry and Physics, 16, 3345–3368, https://doi.org/10.5194/acp-16-3345-2016, 2016.

Clapp, C. E. and Anderson, J. G.: Modeling the Effect of Potential Nitric Acid Removal During Convective Injection of Water Vapor Over the Central United States on the Chemical Composition of the Lower Stratosphere, Journal of Geophysical Research: Atmospheres, 124, 9743–9770, https://doi.org/10.1029/2018JD029703, 2019.

Cooper, O. R., Stohl, A., Trainer, M., Thompson, A. M., Witte, J. C., Oltmans, S. J., Morris, G., Pickering, K. E., Crawford, J. H., Chen, G., Cohen, R. C., Bertram, T. H., Wooldridge, P., Perring, A., Brune, W. H., Merrill, J., Moody, J. L., Tarasick, D., Nédélec, P., Forbes, G., Newchurch, M. J., Schmidlin, F. J., Johnson, B. J., Turquety, S., Baughcum, S. L., Ren, X., Fehsenfeld, F. C., Meagher, J. F., Spichtinger, N., Brown, C. C., McKeen, S. A., McDermid, I. S., and Leblanc, T.: Large upper tropospheric ozone enhancements above midlatitude North America during summer: In situ evidence from the IONS and MOZAIC ozone measurement network, Journal of Geophysical Research: Atmospheres, 111, https://doi.org/10.1029/2006JD007306, 2006.

Dee, D. P., Uppala, S. M., Simmons, A. J., Berrisford, P., Poli, P., Kobayashi, S., Andrae, U., Balmaseda, M. A., Balsamo, G., Bauer, P., Bechtold, P., Beljaars, A. C. M., van de Berg, L., Bidlot, J., Bormann, N., Delsol, C., Dragani, R., Fuentes, M., Geer, A. J., Haimberger, L., Healy, S. B., Hersbach, H., Holm, E. V., Isaksen, L., Kallberg, P., Koehler, M., Matricardi, M., McNally, A. P., Monge-Sanz, B. M., Morcrette, J.-J., Park, B.-K., Peubey, C., de Rosnay, P., Tavolato, C., Thepaut, J.-N., and Vitart, F.: The ERA-Interim reanalysis: configuration and performance of the data assimilation system, Q. J. R. Meteorol. Soc., 137, 553–597, https://doi.org/10.1002/qj.828, 2011.

Dessler, A. E. and Sherwood, S. C.: Effect of convection on the summertime extratropical lower stratosphere, J. Geophys. Res., 109, D23301, 2004.

Dethof, A., O'Neill, A., Slingo, J. M., and Smit, H. G. J.: A mechanism for moistening the lower stratosphere involving the Asian summer monsoon, Q. J. R. Meteorol. Soc., 556, 1079–1106, 1999.

Dunkerton, T. J.: Evidence of meridional motion in the summer lower stratosphere adjacent to monsoon regions, J. Geophys. Res., 100, 16,675–16,688, 1995.

Eluszkiewicz, J., Hemler, R., Mahlman, J., Bruhwiler, L., and Takacs, L.: Sensitivity of age-of-air calculations to the choice of advection scheme, J. Atmos. Sci., 57, 3185–3201, 2000.

Fadnavis, S., Semeniuk, K., Schultz, M. G., Kiefer, M., Mahajan, A., Pozzoli, L., and Sonbawane, S.: Transport pathways of peroxyacetyl nitrate in the upper troposphere and lower stratosphere from different monsoon systems during the summer monsoon season, Atmospheric Chemistry and Physics, 15, 11 477–11 499, https://doi.org/10.5194/acp-15-11477-2015, 2015.

Fadnavis, S., Roy, C., Chattopadhyay, R., Sioris, C. E., Rap, A., Müller, R., Kumar, K. R., and Krishnan, R.: Transport of trace gases via eddy shedding from the Asian summer monsoon anticyclone and associated impacts on ozone heating rates, Atmospheric Chemistry and Physics, 18, 11 493–11 506, https://doi.org/10.5194/acp-18-11493-2018, 2018.

Fu, R., Hu, Y., Wright, J. S., Jiang, J. H., Dickinson, R. E., Chen, M., Filipiak, M., Read, W. G., Waters, J. W., and Wu, D. L.: Short circuit of water vapor and polluted air to the global stratosphere by convective transport over the Tibetan Plateau, Proceedings of the National Academy of Sciences, 103, 5664–5669, https://doi.org/10.1073/pnas.0601584103, 2006.

Fueglistaler, S. and Haynes, P. H.: Control of interannual and longer-term variability of stratospheric water vapor, J. Geophys. Res., 110, D24108, https://doi.org/10.1029/2005JD006019, 2005.

Fueglistaler, S., Dessler, A. E., Dunkerton, T. J., Folkins, I., Fu, Q., and Mote, P. W.: Tropical tropopause layer, Rev. Geophys., 47, RG1004, https://doi.org/10.1029/2008RG000267, 2009.

Garny, H. and Randel, W. J.: Transport pathways from the Asian monsoon anticyclone to the stratosphere, Atmospheric Chemistry and Physics, 16, 2703–2718, https://doi.org/10.5194/acp-16-2703-2016, 2016.

Gettelman, A., ~~Fujiwara, P. M. d. F., Fu, Q., Vömel, H., Gohar, L. K., Johanson, C~~Kinnison, D., Dunkerton, T. J., and ~~Aaammerman, M~~Brasseur, G. P.: ~~Radiation balance of the tropical tropopause layer~~Impact of monsoon circulations on the upper troposphere and lower stratosphere, J. Geophys. Res., 109, ~~, 2004~~D22101, https://doi.org/10.1029/2004JD004878, 2004.

Glatthor, N., Hö~~–~~

~~Gettelman, A., Kinnison, D., Dunkerton~~pfner, M., Stiller, G. P., von Clarmann, T.~~J., and Brasseur, G. P~~, Funke, B., Lossow, S., Eckert, E., Grabowski, U., Kellmann, S., Linden, A., A. Walker, K., and Wiegele, A.: ~~Impact of monsoon circulations on~~ Seasonal and interannual variations in HCN amounts in the upper troposphere and lower stratosphere observed by MIPAS, Atmospheric Chemistry and Physics, 15, 563–582, https://doi.org/10.5194/acp-15-563-2015, 2015.

Gottschaldt, K.-D., Schlager, H., Baumann, R., Cai, D. S., Eyring, V., Graf, P., Grewe, V., J~~J. Geophys.Res., 109, D22101, , 2004~~öckel, P., Jurkat-Witschas, T., Voigt, C., Zahn, A., and Ziereis, H.: Dynamics and composition of the Asian summer monsoon anticyclone~~.~~, Atmospheric Chemistry and Physics, 18, 5655–5675, https://doi.org/10.5194/acp-18-5655-2018, 2018.

Haynes, P. and Shuckburgh, E.: Effective diffusivity as a diagnostic of atmospheric transport, 2, Troposphere and lower stratosphere, J. Geophys. Res., 105, 22 795–22 810, 2000.

Höpfner, M., Ungermann, J., Borrmann, S., Wagner, R., Spang, R., Riese, M., Stiller, G., Appel, O., Batenburg, A. M., Bucci, S., Cairo, F., Dragoneas, A., Friedl-Vallon, F., Hünig, A., Johansson, S., Krasauskas, L., Legras, B., Leisner, T., Mahnke, C., Möhler, O., Molleker, S., Müller, R., Neubert, T., Orphal, J., Preusse, P., Rex, M., Saathoff, H., Stroh, F., Weigel, R., and Wohltmann, I.: Ammonium nitrate particles formed in upper troposphere from ground ammonia sources during Asian monsoons, 12, 608–612, https://doi.org/10.1038/s41561-019-0385-8, 2019.

James, R., Bonazzola, M., Legras, B., Surbled, K., and Fueglistaler, S.: Water vapor transport and dehydration above convective outflow during Asian monsoon, Geophys. Res. Lett., 35, L20810, https://doi.org/10.1029/2008GL035441, 2008.

Konopka, P., Steinhorst, H.-M., Grooß, J.-U., Günther, G., Müller, R., Elkins, J. W., Jost, H.-J., Richard, E., Schmidt, U., Toon, G., and McKenna, D. S.: Mixing and Ozone Loss in the 1999-2000 Arctic Vortex: Simulations with the 3-dimensional Chemical Lagrangian Model of the Stratosphere (CLaMS), J. Geophys. Res., 109, D02315, https://doi.org/10.1029/2003JD003792, 2004.

Konopka, P., Ploeger, F., Tao, M., Birner, T., and Riese, M.: Hemispheric asymmetries and seasonality of mean age of air in the lower stratosphere: Deep versus shallow branch of the Brewer-Dobson circulation, J. Geophys. Res., 120, 2053–2066, https://doi.org/10.1002/2014JD022429, 2015.

Konopka, P., Ploeger, F., Tao, M., and Riese, M.: Regionally Resolved Diagnostic of Transport: A Simplified Forward Model for CO2, Journal of the Atmospheric Sciences, 74, 2689–2700, https://doi.org/10.1175/JAS-D-16-0367.1, 2017.

Li, D., Vogel, B., Müller, R., Bian, J., Günther, G., Li, Q., Zhang, J., Bai, Z., Vömel, H., and Riese, M.: High tropospheric ozone in Lhasa within the Asian summer monsoon anticyclone in 2013: influence of convective transport and stratospheric intrusions, Atmospheric Chemistry and Physics, 18, 17 979–17 994, https://doi.org/10.5194/acp-18-17979-2018, 2018.

~~Liang~~

Li, Q., ~~Jaeglé,~~ Jacob, D. J., Park, R., Wang, Y., Heald, C. L., ~~Jaffe, D. A., Weiss-Penzias, P., Heckman, A., and Snow, J. A~~Hudman, R., Yantosca, R. M., Martin, R. V., and Evans, M.: ~~Long-range transport of Asian pollution to the northeast Pacific: Seasonal variations and transport pathways of carbon monoxide~~North American pollution outflow and the trapping of convectively lifted pollution by upper-level anticyclone, Journal of Geophysical Research: Atmospheres, ~~109, , 2004.~~ 110, https://doi.org/10.1029/2004JD005039, 2005.

Livesey, N. J., Read, W. G., Wagner, P. A., Froidevaux, L., Lambert, A., Manney, G. L., Valle, L. F. M., Pumphrey, H. C., Santee, M. L., Schwartz, M. J., Wang, S., Fuller, R. A., Jarnot, R. F., Knosp, B. W., and Martinez, E.: Version 4.2x Level 2 data quality and description document, https://mls.jpl.nasa.gov/data/v4-2_data_quality_document.pdf, 2018.

McKenna, D. S., Konopka, P., Grooß, J.-U., Günther, G., Müller, R., Spang, R., Offermann, D., and Orsolini, Y.: A new Chemical Lagrangian Model of the Stratosphere (CLaMS): 1. Formulation of advection and mixing, J. Geophys. Res., 107, 4309, https://doi.org/10.1029/2000JD000114, 2002.

Molnar, P., England, P., and Martinod, J.: Mantle dynamics, uplift of the Tibetan Plateau, and the Indian Monsoon, Reviews of Geophysics, 31, 357–396, https://doi.org/10.1029/93RG02030, 1993.

Mote, P. W., Rosenlof, K. H., McIntyre, M. E., Carr, E. S., Gille, J. G., Holton, J. R., Kinnersley, J. S., Pumphrey, H. C., Russell III, J. M., and Waters, J. W.: An atmospheric tape recorder: The imprint of tropical tropopause temperatures on stratospheric water vapor, J. Geophys. Res., 101, 3989 – 4006, 1996.

Nützel, M., Podglajen, A., Garny, H., and Ploeger, F.: Quantification of water vapour transport from the Asian monsoon to the stratosphere, Atmospheric Chemistry and Physics, 19, 8947–8966, https://doi.org/10.5194/acp-19-8947-2019, 2019.

Orbe, C., Holzer, M., Polvani, L. M., and Waugh, D.: Air-mass origin as a diagnostic of tropospheric transport, J. Geophys. Res., 118, 1459–1470, https://doi.org/10.1002/jgrd.50133, 2013.

Pan, L. L., Honomichl, S. B., Kinnison, D. E., Abalos, M., Randel, W. J., Bergman, J. W., and Bian, J.: Transport of chemical tracers from the boundary layer to stratosphere associated with the dynamics of the Asian summer monsoon, Journal of Geophysical Research: Atmospheres, 121, 14,159–14,174, https://doi.org/10.1002/2016JD025616, 2016.

Park, M., Randel, W. J., Emmons, L. K., Bernath, P. F., Walker, K. A., and Boone, C. D.: Chemical isolation in the Asian monsoon anticyclone observed in Atmospheric Chemistry Experiment (ACE-FTS) data, Atmos. Chem. Phys., 8, 757–764, 2008.

Park, M., Randel, W. J., Emmons, L. K., and Livesey, N. J.: Transport pathways of carbon monoxide in the Asian summer monsoon diagnosed from Model of Ozone and Related Tracers (MOZART), J. Geophys. Res., 114, D08303, https://doi.org/10.1029/2008JD010621, 2009.

Pillai, P. A. and Mohankumar, K.: Local Hadley circulation over the Asian monsoon region associated with the Tropospheric Biennial Oscillation, Theoretical and Applied Climatology, 91, 171–179, https://doi.org/10.1007/s00704-007-0305-5, 2008.

Ploeger, F., Konopka, P., Günther, G., Grooß, J.-U., and Müller, R.: Impact of the vertical velocity scheme on modeling transport across the tropical tropopause layer, J. Geophys. Res., 115, D03301, https://doi.org/10.1029/2009JD012023, 2010.

Ploeger, F., Günther, G., Konopka, P., Fueglistaler, S., Müller, R., Hoppe, C., Kunz, A., Spang, R., Grooß, J.-U., and Riese, M.: Horizontal water vapor transport in the lower stratosphere from subtropics to high latitudes during boreal summer, J. Geophys. Res., 118, 8111–8127, https://doi.org/10.1002/jgrd.50636, 2013.

Ploeger, F., ~~Riese, M., Haenel, F~~Gottschling, C., Griessbach, S., Grooß, J.-U., Guenther, G., Konopka, P., Müller, R., ~~and Stiller, G~~Riese, M., Stroh, F., Tao, M., Ungermann, J., Vogel, B., and von Hobe, M.: ~~Variability of stratospheric mean age of air and of the local effects of residual circulation and eddy mixing~~A potential vorticity-based determination of the transport barrier in the Asian summer monsoon anticyclone, ~~J. Geophys. Res., 120, 716–733,~~ Atmospheric Chemistry and Physics, 15, 13 145–13 159, https://doi.org/10.5194/acp-15-13145-2015, 2015.

Ploeger, F., Konopka, P., Walker, K., and Riese, M.: Quantifying pollution transport from the Asian monsoon anticyclone into the lower stratosphere, Atmos. Chem. Phys., 16, 7055–7066, https://doi.org/10.5194/acp-17-7055-2017, 2017.

Ploeger, F., Legras, B., Charlesworth, E., Yan, X., Diallo, M., Konopka, P., Birner, T., Tao, M., Engel, A., and Riese, M.: How robust are stratospheric age of air trends from different reanalyses?, Atmospheric Chemistry and Physics, 19, 6085–6105, https://doi.org/10.5194/acp-19-6085-2019, 2019.

Pommrich, R., Müller, R., Grooß, J.-U., Konopka, P., Ploeger, F., Vogel, B., Tao, M., Hoppe, C. M., Günther, G., Spelten, N., Hoffmann, L., Pumphrey, H.-C., Viciani, S., D'Amato, F., Volk, C. M., Hoor, P., Schlager, H., and Riese, M.: Tropical troposphere to stratosphere transport of carbon monoxide and long-lived trace species in the Chemical Lagrangian Model of the Stratosphere (CLaMS), Geoscientific Model Development, 7, 2895–2916, https://doi.org/10.5194/gmd-7-2895-2014, 2014.

Popovic, J. M. and Plumb, R. A.: Eddy Shedding from the Upper-Tropospheric Asian Monsoon Anticyclone, Journal of the Atmospheric Sciences, 58, 93–104, https://doi.org/10.1175/1520-0469(2001)058<0093:ESFTUT>2.0.CO;2, 2001.

Poshyvailo, L., Müller, R., Konopka, P., Günther, G., Riese, M., Podglajen, A., and Ploeger, F.: Sensitivities of modelled water vapour in the lower stratosphere: temperature uncertainty, effects of horizontal transport and small-scale mixing, Atmospheric Chemistry and Physics, 18, 8505–8527, 2018.

Randel, W. and Jensen, E.: Physical processes in the tropical tropopause layer and their role in a changing climate, Nature Geoscience, 6, 169–176, https://doi.org/10.1038/ngeo1733, 2013.

Randel, W. J. and Park, M.: Deep convective influence on the Asian summer monsoon anticyclone and associated tracer variability observed with Atmospheric Infrared Sounder (AIRS), J. Geophys. Res., 111, D12314, https://doi.org/10.1029/2005JD006490, 2006.

Randel, W. J., Wu, F., Gettelman, A., Russell, J., Zawodny, J., and Oltmans, S.: Seasonal variation of water vapor in the lower stratosphere observed in Halogen Occultation Experiment data, J. Geophys. Res., 106, D13, https://doi.org/10.1029/2001JD900048, 2001.

Randel, W. J., Park, M., Emmons, L., Kinnison, D., Bernath, P., Walker, K. A., Boone, C., and Pumphrey, H.: Asian Monsoon Transport of Pollution to the Stratosphere, Science, 328, 611–613, https://doi.org/10.1126/science.1182274, 2010.

Randel, W. J., Moyer, E., Park, M., Jensen, E., Bernath, P., Walker, K., and Boone, C.: Global variations of HDO and HDO/$H_2O$ ratios in the upper troposphere and lower stratosphere derived from ACE–FTS satellite measurements, J. Geophys. Res., 117, D06303, https://doi.org/10.1029/2011JD016632, 2012.

Randel, W. J., Zhang, K., and Fu, R.: What controls stratospheric water vapor in the NH summer monsoon regions?, Journal of Geophysical Research: Atmospheres, 120, 7988–8001, https://doi.org/10.1002/2015JD023622, 2015.

Riese, M., Ploeger, F., Rap, A., Vogel, B., Konopka, P., Dameris, M., and Forster, P.: Impact of uncertainties in atmospheric mixing on simulated UTLS composition and related radiative effects, J. Geophys. Res., 117, D16305, https://doi.org/10.1029/2012JD017751, 2012.

Robrecht, S., Vogel, B., Grooß, J.-U., Rosenlof, K., Thornberry, T., Rollins, A., Krämer, M., Christensen, L., and Müller, R.: Mechanism of ozone loss under enhanced water vapour conditions in the mid-latitude lower stratosphere in summer, Atmospheric Chemistry and Physics, 19, 5805–5833, https://doi.org/10.5194/acp-19-5805-2019, 2019.

Rolf, C., Vogel, B., Hoor, P., Afchine, A., Günther, G., Krämer, M., Müller, R., Müller, S., Spelten, N., and Riese, M.: Water vapor increase in the lower stratosphere of the Northern Hemisphere due to the Asian monsoon anticyclone observed during the TACTS/ESMVal campaigns, Atmospheric Chemistry and Physics, 18, 2973–2983, https://doi.org/10.5194/acp-18-2973-2018, 2018.

Rosenlof, K. H.: Seasonal cycle of the residual mean meridional circulation in the stratosphere, J. Geophys. Res., 100, 5173 – 5191, 1995.

Rosenlof, K. H., Tuck, A. F., Kelly, K. K., Russell III, J. M., and McCormick, M. P.: Hemispheric asymmetries in the water vapor and inferences about transport in the lower stratosphere, J. Geophys. Res., 102, 13 213–13 234, https://doi.org/10.1029/97JD00873, 1997.

Roy, I.: Ozone Depletion in the Stratosphere, pp. 203–205, Springer International Publishing, Cham, https://doi.org/10.1007/978-3-319-77107-6_17, 2018.

Santee, M. L., Manney, G. L., Livesey, N. J., Schwartz, M. J., Neu, J. L., and Read, W. G.: A comprehensive overview of the climatological composition of the Asian summer monsoon anticyclone based on 10 years of Aura Microwave Limb Sounder measurements, Journal of Geophysical Research: Atmospheres, 122, 5491–5514, https://doi.org/10.1002/2016JD026408, 2017.

Schoeberl, M. R., Douglass, A. R., Zhu, Z. X., and Pawson, S.: A comparison of the lower stratospheric age spectra derived from a general circulation model and two data assimilation systems, J. Geophys. Res., 108, 4113, https://doi.org/10.1029/2002JD002652, 2003.

Schoeberl, M. R., Dessler, A. E., and Wang, T.: Simulation of stratospheric water vapor and trends using three reanalyses, Atmos. Chem. Phys., 12, 6475–6487, https://doi.org/10.5194/acp-12-6475-2012, 2012.

Schwartz, M. J., Read, W. G., Santee, M. L., Livesesy, N. J., Froidevaux, L., Lamert, A., and Manney, G. L.: Convectively injected water vapor in the North American summer lowermost stratosphere, Geophys. Res. Lett., 40, 2316–2321, https://doi.org/10.1002/grl.50421, 2013.

Seviour, W. J. M., Butchart, N., and Hardiman, S. C.: The Brewer-Dobson circulation inferred form ERA-Interim, Q. J. R. Meteorol. Soc., 138, 878–888, 2011.

Solomon, S., Rosenlof, K., Portmann, R., Daniel, J., Davis, S., Sanford, T., and Plattner, G.-K.: Contributions of stratospheric water vapor to decadal changes in the rate of global warming, Science, 327, 1219–1223, https://doi.org/10.1126/science.1182488, 2010.

Tao, M., Konopka, P., Ploeger, F., Yan, X., Wright, J. S., Diallo, M., Fueglistaler, S., and Riese, M.: Multitimescale variations in modeled stratospheric water vapor derived from three modern reanalysis products, Atmospheric Chemistry and Physics, 19, 6509–6534, https://doi.org/10.5194/acp-19-6509-2019, 2019.

Tissier, A.-S. and Legras, B.: Convective sources of trajectories traversing the tropical tropopause layer, Atmos. Chem. Phys., 16, 3383–3398, 2016.

Tweedy, O. V., Waugh, D. W., Randel, W. J., Abalos, M., Oman, L. D., and Kinnison, D. E.: The Impact of Boreal Summer ENSO Events on Tropical Lower Stratospheric Ozone, Journal of Geophysical Research: Atmospheres, 123, 9843–9857, https://doi.org/10.1029/2018JD029020, 2018.

Ungermann, J., Ern, M., Kaufmann, M., Müller, R., Spang, R., Ploeger, F., Vogel, B., and Riese, M.: Observations of PAN and its confinement in the Asian summer monsoon anticyclone in high spatial resolution, Atmospheric Chemistry and Physics, 16, 8389–8403, https://doi.org/10.5194/acp-16-8389-2016, 2016.

Vernier, J.-P., Thomason, L. W., and Kar, J.: CALIPSO detection of an Asian tropopause aerosol layer, Geophys. Res. Lett., 38, L07804, https://doi.org/10.1029/2010GL046614, 2011.

Vernier, J. P., Fairlie, T. D., Natarajan, M., Wienhold, F. G., Bian, J., Martinsson, B. G., Crumeyrolle, S., Thomason, L. W., and Bedka, K. M.: Increase in upper tropospheric and lower stratospheric aerosol levels and its potential connection with Asian pollution, J. Geophys. Res., https://doi.org/10.1002/2014JD022372, 2015.

Vernier, J.-P., Fairlie, T. D., Deshler, T., Venkat Ratnam, M., Gadhavi, H., Kumar, B. S., Natarajan, M., Pandit, A. K., Akhil Raj, S. T., Hemanth Kumar, A., Jayaraman, A., Singh, A. K., Rastogi, N., Sinha, P. R., Kumar, S., Tiwari, S., Wegner, T., Baker, N., Vignelles, D., Stenchikov, G., Shevchenko, I., Smith, J., Bedka, K., Kesarkar, A., Singh, V., Bhate, J., Ravikiran, V., Durga Rao, M., Ravindrababu, S., Patel, A., Vernier, H., Wienhold, F. G., Liu, H., Knepp, T. N., Thomason, L., Crawford, J., Ziemba, L., Moore, J., Crumeyrolle, S., Williamson, M., Berthet, G., Jégou, F., and Renard, J.-B.: BATAL: The Balloon Measurement Campaigns of the Asian Tropopause Aerosol Layer, Bulletin of the American Meteorological Society, 99, 955–973, 2018.

Vogel, B., Günther, G., Müller, R., Grooß, J.-U., Hoor, P., Krämer, M., Müller, S., Zahn, A., and Riese, M.: Fast transport from Southeast Asia boundary layer sources to northern Europe: rapid uplift in typhoons and eastward eddy shedding of the Asian monsoon anticyclone, Atmos. Chem. Phys., 14, 12 745–12 762, https://doi.org/10.5194/acp-14-12745-2014, 2014.

Vogel, B., Günther, G., Müller, R., Grooß, J.-U., Afchine, A., Bozem, H., Hoor, P., Krämer, M., Müller, S., Riese, M., Rolf, C., Spelten, N., Stiller, G. P., Ungermann, J., and Zahn, A.: Long-range transport pathways of tropospheric source gases originating in Asia into the northern lower stratosphere during the Asian monsoon season 2012, Atmospheric Chemistry and Physics, 16, 15 301–15 325, 2016.

Vogel, B., Müller, R., Günther, G., Spang, R., Hanumanthu, S., Li, D., Riese, M., and Stiller, G. P.: Lagrangian simulations of the transport of young air masses to the top of the Asian monsoon anticyclone and into the tropical pipe, Atmospheric Chemistry and Physics, 19, 6007–6034, https://doi.org/10.5194/acp-19-6007-2019, 2019.

Wang, T., Randel, W. J., Dessler, A. E., Schoeberl, M. R., and Kinnison, D. E.: Trajectory model simulations of ozone ($O_3$) and carbon monoxide (CO) in the lower stratosphere, Atmospheric Chemistry and Physics, pp. 7135–7147, https://doi.org/10.5194/acp-14-7135-2014, 2014.

Wright, J. S. and Fueglistaler, S.: Large differences in reanalyses of diabatic heating in the tropical upper troposphere and lower stratosphere, Atmos. Chem. Phys., 13, 9565–9576, https://doi.org/10.5194/acp-13-9565-2013, 2013.

Wright, J. S., Fu, R., Fueglistaler, S., Liu, Y. S., and Zhang, Y.: The influence of summertime convection over Southeast Asia on water vapor in the tropical stratosphere, J. Geophys. Res., 116, D12302, https://doi.org/10.1029/2010JD015416, 2011.

Yan, X., Konopka, P., Ploeger, F., Tao, M., Müller, R., Santee, M. L., Bian, J., and Riese, M.: El Niño Southern Oscillation influence on the Asian summer monsoon anticyclone, Atmospheric Chemistry and Physics, pp. 8079–8096, https://doi.org/10.5194/acp-18-8079-2018, 2018.

Yu, P., Rosenlof, K. H., Liu, S., Telg, H., Thornberry, T. D., Rollins, A. W., Portmann, R. W., Bai, Z., Ray, E. A., Duan, Y., Pan, L. L., Toon, O. B., Bian, J., and Gao, R.-S.: Efficient transport of tropospheric aerosol into the stratosphere via the Asian summer monsoon anticyclone, Proceedings of the National Academy of Sciences, pp. 6972–6977, https://doi.org/10.1073/pnas.1701170114, 2017.

| | | 350−360 K | | | 370−380 K | | |
|---|---|---|---|---|---|---|---|
| Destination | | LS-NH | LS-SH | TrP | LS-NH | LS-SH | TrP |
| ASM | MC | 18 % | 6 % | 7 % | 22 % | 2 % | 4 % |
| | ME | 2.5‰ | 0.4‰ | 0.7‰ | 9‰ | 0.35‰ | 1.45‰ |
| | FC | 2.4 % | 3.2 % | 4.8 % | 1.2 % | 1.2 % | 3 % |
| | FE | 0.5‰ | 0.2‰ | 0.55‰ | 0.6‰ | 0.2‰ | 0.89‰ |
| | TT | 3 months | 6 months | 8.5 months | 2.5 months | 5.5 months | 8 months |
| NASM | MC | 10 % | 2.5 % | 2.5 % | 21 % | 1 % | 2 % |
| | ME | 2.6‰ | 0.25‰ | 0.4‰ | 14‰ | 0.32‰ | 0.95‰ |
| | FC | 1 % | 1.3 % | 2 % | 0.5 % | 0.6 % | 1.3 % |
| | FE | 0.3‰ | 0.15‰ | 0.33‰ | 0.4‰ | 0.18‰ | 0.6‰ |
| | TT | 2 months | 6 months | 9 months | 2 months | 5.5 months | 8 months |
| Tropics | MC | 17 % | 14 % | 10 % | 22 % | 14.5 % | 12 % |
| | ME | 0.8‰ | 0.3‰ | 0.32‰ | 3.5‰ | 1.1‰ | 1.46‰ |
| | FC | 1.2 % | 3.8 % | 5 % | 1.2 % | 3.5 % | 5 % |
| | FE | 0.1‰ | 0.1‰ | 0.18‰ | 0.2‰ | 0.24‰ | 0.65‰ |
| | TT | 2.5 months | 4.5 months | 8 months | 2.5 months | 4 months | 7.5 months |

**Table 3.** The maximum contribution (MC, in %), maximum efficiency (ME, in ‰), final (at the end of simulation period from each year) contribution (FC, in %), final efficiency (FE, in ‰) and transit time (TT, in month) from the three source regions (ASM, NASM, and Tropics) to the three destination regions (LS-NH, LS-SH, and TrP) based on the CLaMS-EI simulations.